1962

The influence of bench geometry on blasting effects for vertical cylindrical charges

Thomas E. Pearse

THE INFLUENCE OF BENCH GEOMETRY ON BLASTING EFFECTS FOR VERTICAL CYLINDRICAL CHARGES

BY

THOMAS E. PEARSE

A

THESIS

submitted to the faculty of the

SCHOOL OF MINES AND METALLURGY OF THE UNIVERSITY OF MISSOURI

in partial fulfillment of the work required for the

Degree of

MASTER OF SCIENCE IN MINING ENGINEERING

Rolla, Missouri

1962

Approved by

Richard L. Ash (advisor) R. E. Oeffner

H. M. Zern L. C. Christianson

ABSTRACT

Blasting phenomena are affected by many factors. Previous investigators have studied many of these factors, however, the influence of charge length and explosive detonation velocity have apparently not been thoroughly examined.

It was found by this investigation that the detonation pressure of a commercial explosive is closely controlled by the detonation velocity. The detonation velocity, in turn, will largely determine the necessary blast geometry that can be successfully employed. Relationships were derived between the detonation velocity, in relation to the rock energy propagation velocity, and blast geometry for both bottom and collar primed blasts.

The resultant force magnitude and direction at a point in the medium was found to be influenced by the charge length and the velocity ratio. A graphical analysis of the forces in the medium indicated that the direction of the resultant forces along the reflected pulse front is not perpendicular to this wave front.

Observed blasting phenomena appear to substantiate the theoretical investigation.

STATEMENT OF THE PROBLEM

This investigation was conducted to determine the importance of charge length and explosive velocity on blast dimensioning. The theoretical investigation was restricted to single, vertical blast-holes in a homogeneous, isotropic material. A study of field blasting practices was conducted to enable the correlation of theoretical considerations with blasting techniques as are used when blasting under actual field conditions.

ACKNOWLEDGEMENT

The writer wishes to express his appreciation to Professor R. L. Ash, of the Mining Engineering Department, Missouri School of Mines and Metallurgy, who suggested the problem and offered continued assistance and guidance throughout the investigation. Appreciation is due to Dr. H. M. Zenor, of the Mining Engineering Department, Missouri School of Mines and Metallurgy, for his valuable criticism of the manuscript. Professor R. F. Bruzewski, of the Mining Engineering Department, Missouri School of Mines and Metallurgy, assisted the author in preparing the photographs.

The Atlas Powder Company provided the author with the sequence photographs of field blasts.

TABLE OF CONTENTS

PAGE

ABSTRACT i

STATEMENT OF THE PROBLEM ii

ACKNOWLEDGEMENT iii

TABLE OF CONTENTS iv

LIST OF TABLES vi

LIST OF ILLUSTRATIONS vii

CHAPTER PAGE

I. INTRODUCTION 1

II. BLASTING MECHANISMS 5

Hydrodynamic and Thermodynamic Theories of Detonation 5

Explosive Energy Transmission Through Rock. 8

Effect of a Single Free Face - Point Charge 12

Effect of Multiple Free Faces - Point Charge 14

Effect of Multiple Free Faces - Cylindrical Charge 17

III. INFLUENCE OF CHARGE LENGTH AND VELOCITY RATIO ON BLAST DIMENSIONING 20

The Dependency of the Detonation Pressure on Density and Velocity 20

Influence of Initiator Position 24

Bottom Priming 25

CHAPTER PAGE

Collar Priming 29

Effect of Charge Length on Stress Distribution 32

IV. FIELD BLASTING TECHNIQUES 40

Experimental Investigation 40

Correlative Survey of Blasting Practices. . 47

V. SUMMARY AND CONCLUSIONS. 57

VI. PROPOSED AREAS FOR FUTURE INVESTIGATION . . . 61

APPENDIXES

A. Table of Symbols 65

B. Derivation of Time-Stress Balancing Relationships 67

C. Graphical Method for Determining the Magnitude and Direction of the Resultant Forces at Different Points in a Medium from Detonation of a Cylindrical Charge 73

D. Sequence Photographs of Field Bench Blasts Using Large Diameter Vertical Blast-holes . 81

BIBLIOGRAPHY 95

VITA 98

LIST OF TABLES

TABLE		PAGE
I.	FREQUENCY DISTRIBUTION OF STEMMING RATIO: FIELD PRACTICES	50
II.	FREQUENCY DISTRIBUTION OF SUBDRILLING RATIO: FIELD PRACTICES	53
III.	SPEED OF TRANSMISSION OF LONGITUDINAL WAVES IN ROCKS	54

LIST OF ILLUSTRATIONS

FIGURE		PAGE
1.	Schematic Representation of Particle Displacement by Pressure Pulse	9
2.	Mechanism of Multiple Slabbing	15
3.	Fracture Formation Resulting From Interaction of Tensile Pulses.	16
4.	Distribution of Pressure Wave Fronts in Rock .	19
5.	Density - Detonation Pressure Relationships for Commercial Explosives	21
6.	Velocity - Detonation Pressure Relationships for Commercial Explosives	22
7.	Velocity - Density Relationships for Commercial Explosives	23
8.	Minimum L/B Ratio for Bottom Priming	27
9.	Maximum L/B Ratio for Collar Priming	31
10.	Force Distribution Along Reflected Wave Front, for Ve/Vr = ½	35
11.	Force Distribution Along Reflected Wave Front, for Ve/Vr = 1	36
12.	Force Distribution Along Reflected Wave Front, for Ve/Vr = 2	37
13.	Design Details of Test Number 1	42
14.	Design Details of Test Number 2	45
15.	Stemming Ratios: Field Practices	48
16.	Subdrilling Ratios: Field Practices	52

FIGURE PAGE

17. L/B vs. Ve/Vr: Field Practices 55
18. Vertical Bench Section Illustrating Blast Geometry 69
19. Simplified Distribution of Pressure Wave Front: Bottom Primed - Ve/Vr = 1 76
20. Peak Pressure Decay with Travel Distance. . . . 78
21. Graphical Determination of Force Magnitude at a Point in Rock. 79

PLATE PAGE

1. Test Number 1 Before Blasting 42
2. Test Number 1 After Blasting 43
3. Fractures Formed by Test Number 1 43
4. Test Number 2 Before Blasting 45
5. Test Number 2 After Blasting 46
6. Crater Formed in Horizontal Free Face From Test Number 2 46
7. Corner Fracture Formation 83
8. Blasting Sequence for Bottom Priming 87
9. Sequence for Collar Priming (Inadequate Stemming) 91

CHAPTER I

INTRODUCTION

In an effort to aid in the solution of certain unexplained phenonema observed during actual field blasting a thorough search was conducted of all available literature on the subject. However, very little information was found that related the length of an explosive charge to bench geometry, a condition that exists for all blasting in the field. The assumption used by many investigators was that the charge has a spherical shape. This assumption serves to limit the number of variables involved when an analysis is to be made, but, it oversimplifies the actual conditions and does not satisfactorily explain effects as observed.

Some of the more important contributions toward a solution of the problem of bench geometry were presented by Hino (12, p. 122). Hino determined, by an analysis of the interaction of shock waves generated from a point charge, a relationship between the maximum height of bench (L) that can be used for a particular burden dimension. The burden (B) is generally considered the distance from the explosive charge to the nearest free face. From the analysis he deduced that the bench height could be as much as twice the burden dimension. This conclusion, however, does not exist for many actual field conditions. Other investigators generally overlook

the relationship of bench geometry and evaluate results based on only one free surface.

In relating blast effects and bench geometry another investigator, Pearse (24, p. 22), and Hino (12, p. 3) independently proposed equations relating the burden dimension to the tensile strength of the rock (S_t) and to the detonation pressure of the explosive (P_d). Their reasoning was based on the fact that most rocks are weakest under tensile stressing. Their approach to the problem was entirely different. Hino assumed that the rock is broken predominantly by tensile slabbing from a wave reflected from a free face (Figure 2). Pearse assumed that rock is broken by radial expansion from the initial compressive pulse (Figure 1), and that the explosive detonation velocity has an infinite value. Curiously, the form for both equations can be expressed by the same simple relationship:

$$B = K\, d_e \left(\frac{P_d}{S_t}\right)^{\beta} \qquad (1)$$

where: d_e - diameter of explosive charge

K - constant dependent on explosive type and amount

Hino, $K = 1.0$

Pearse, $K = 0.7$ to 1.0

β - absorption constant dependent on rock type

Hino, $\beta = 0.5$ for point charges, 0.67 for cylindrical charges

Pearse, $\beta = 0.5$

(Refer to Appendix A for a definition of the symbols.) The similarity of the two equations is remarkable, even though they are based on different basic assumptions. It should be noted that only one free face was considered in both derivations.

Another theory, proposed by Livingston (18), attempted to explain rock breakage by explosive loading in terms of the rate of energy transfer in the rock. Experimentally he found that rock breakage patterns changed regularly when the burden for a particular amount and type of explosive was uniformly varied. Livingston was able to classify four major breakage ranges, each of which was characterized by a distinct response to explosive action. The basis for his theory was the shape of the crater formed by the detonation of a particular type and amount of explosive at various depths below a reflection boundary (14). The charge shape must be maintained as nearly spherical as possible to insure the formation of a spherically diverging pressure wave. Relationships between the type of rock and the amount of explosive used can then be established and used as an aid in blast design (5).

An expression proposed by Kochanowsky (16, p. 864), based on blasting with point charges, related the charge size to the burden dimension as follows:

$$W = CB^2 + C'B^3 \qquad (2)$$

The "C" relates to the strength of the rock while the "C'" is applicable to the force necessary to move the broken rock a certain distance. Geometric relationships of the blast design are considered in the two terms of the equation. Langefors (17, p. 220) proposed an expression that was very similar to that of Kochanowsky.

An expression proposed by O. Anderson (1, p. 116), is as follows:

$$B = (aL)^{\frac{1}{2}} \qquad (3)$$

The expression was derived emperically from field observations but considers neither the rock characteristics nor those of the explosive. Any changes in either the rock or the explosive types should not necessitate any corresponding changes in the blast design according to the expression.

The aforementioned studies, as well as work done by many others, all appear to indicate that relationships determined to date do not explain the phenomena observed visually, or photographically, of many actual blasts. It becomes apparent that the effects of explosive charge length, explosive and rock energy-propagation velocities, and bench geometry have not yet been evaluated. It would seem advantageous, then, to investigate those relationships and their relative importance in the blasting process.

CHAPTER II

BLASTING MECHANISMS

In order to investigate the overall blasting process it is necessary to isolate and study each basic mechanism separately. In this manner the relative importance of each may be ascertained. It would be necessary in the first analysis to determine the energy potential of an explosive, and then investigate its physical action on the material being blasted. For simplicity the material being blasted would be assumed to be homogeneous and isotropic, i.e., massive and having a uniform density with no stratification, jointing, or similar structural discontinuities.

Hydrodynamic and Thermodynamic Theories of Detonation

A characteristic of many explosives is that they detonate, which is a process whereby energy is released. The potential work ability of an explosive can be related to the propagation of the detonation wave through the explosive, which is characterized by several properties: 1. a rapid rise in pressure at the detonation front, 2. the formation of very high pressures (13), and 3. a supersonic velocity of wave propagation (6, p. 177). An expression relating the detonation velocity (V_e) and the sonic velocity (V_c) of the explosive is as follows (8, p.61):

$$V_e = V_s + V_c$$

In a compressive wave the streaming velocity V_s is in the direction of movement of the wave front while it is opposite to the direction of movement in the case of a rarefraction wave.

The hydrodynamic theory, which utilizes principles of the conservation of mass, momentum, and energy across the detonation front, has been used to determine relationships between various blasting parameters. The three following fundamental equations have been derived by use of this theory (23, 32, 34):

$$V_e = V_o \left(\frac{P_d - P_o}{V_o - V}\right)^{\frac{1}{2}} \tag{5}$$

$$V_s = (V_o - V) \left(\frac{P_d - P_o}{V_o - V}\right)^{\frac{1}{2}} \tag{6}$$

$$E = \tfrac{1}{2} (P_d - P_o)(V_o - V) \tag{7}$$

where: V_o - Specific volume of undetonated explosive cc/gm,

V - Specific volume of gaseous products in the detonation head cc/gm,

P_o - Initial explosive pressure,

E - Total energy content.

The above equations, however, cannot be utilized unless the equation of state of the products and the energy equation of the reaction is known. The necessary thermodynamic considerations lead to the following relationships (32, p. 87):

$$V_e = \frac{\gamma+1}{1-\alpha\rho}\left(\frac{nR\ {}^{o}K}{\gamma}\right)^{\frac{1}{2}} \tag{8}$$

$$V_s = \left(\frac{nR\ {}^{o}K}{\gamma}\right)^{\frac{1}{2}} \tag{9}$$

where: $\gamma - 1+\frac{nR}{c_v}$

c_v - Specific heats of gaseous products at constant volume,

n - Number of moles of gaseous products per Kg. of explosive,

R - gas constant,

^{o}K - Temperature,

ρ - Explosive density.

In the above equations, however, the covolume (α) is considered to be constant. Similar expressions have been developed by Clark (7, p. 39) but for which the covolume was not considered to be constant, the covolume being defined as the volume occupied by non-gaseous products. At the high temperatures and pressures existing during detonation the volume of the gas molecules constitutes a substantial portion of the total volume so it should be considered. The covolume may be expressed in terms of the instantaneous density (12, p. 65) as follows:

$$\alpha = \alpha_o - a\rho_o \tag{10}$$

When equations 5, 6, 8, 9, and 10 are combined a general equation for the detonation pressure in terms of the detonation velocity and the initial explosive density can be obtained (12, p. 65,) or,

$$P_d = \frac{V_e\ \rho_o}{K+1}\ (1 - \alpha_o\rho_o + a\ \rho_o^{2}) \tag{11}$$

In the above expression the initial pressure has been

neglected.

Actual experimental measurement of this pressure is very difficult since available materials are not capable of withstanding the intensity of the high pressures involved (13).

Explosive Energy Transmission Through Rock

The very short rise time of the explosive pressure during detonation creates a pressure front in the rock that travels at a velocity dependent on the properties of the rock. Particles ahead of the pressure wave are not disturbed, while those behind the pressure front are set into complex harmonic motion.

If the material is homogeneous and isotropic, the pressure wave from a single point charge will be spherical. Each particle along the wave front is displaced radially from the shot point by the pressure. The magnitude of the displacement along the wave front is the same for all particles. The displacement, however, varies from point to point, producing tangential tension along the compressive wave front. Figure 1 illustrates schematically the particle motion along the wave front that diverges from a point charge.

Near the borehole the generated compressive stress usually exceeds the compressive strength of the rock, and the rock is crushed. Because of the rapid attenuation of the peak stress rock breakage by compression is limited

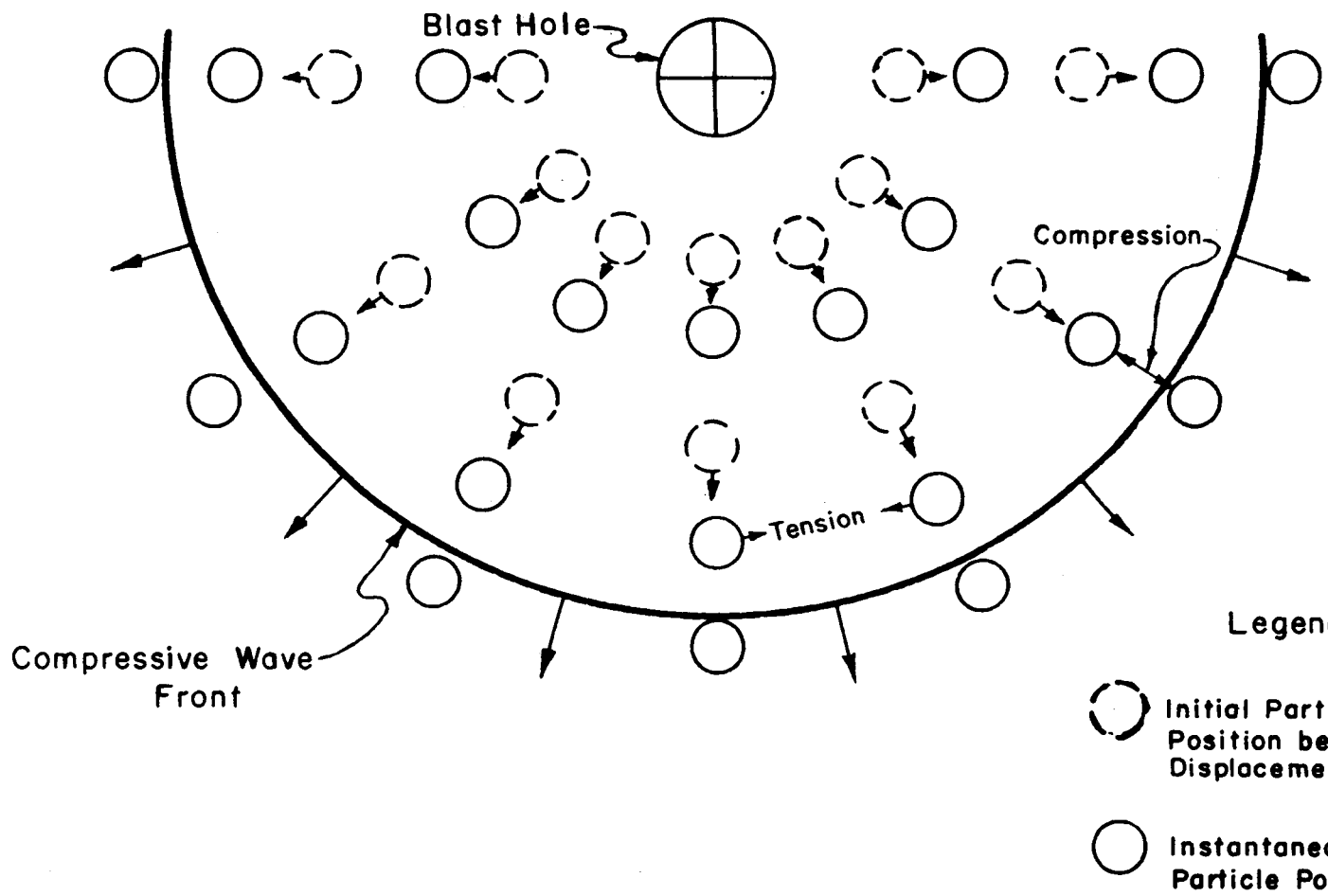

Figure 1. Schematic Representation of Particle Displacement by Pressure Pulse.

to a small region surrounding the borehole. At some distance from the borehole the pressure just equals the compressive strength of the rock and the crushing action ceases. The rock particles beyond this zone are set into motion by the compressive wave and behave elastically, except for viscous and internal frictional effects. The motion is not intense enough to cause any further compressive crushing. However, the radial tensile stress, by exceeding the tensile strength of the rock, causes radial tension cracks to form and propagate outward from the borehole.

The magnitude and direction of the total stress at any point in the rock is determined by the amplitude and pulse shape of the individual stress waves that interact (29). Rock breakage will be most likely to occur where a high level of stress has developed (30). Strain pulse shapes have been recorded experimentally by several investigators (9, 10, 11, 22), and it has been found that they are functions of the rock characteristics, the amount and type of explosive, and the travel distance. As rock often behaves inelasticly during blasting the stress pulse shape is not necessarily similar to that of the strain pulse. According to Hino (12, p. 53), the stress pulse decay can be described by the following equation:

$$P_r = Ke^{-\frac{x}{b}} \qquad (12)$$

The constant K is dependent on the amount and type of explosive, while b is dependent on the rock type. The

constant b was found to have a magnitude near 30, while K ranged from 500 to 1000 in value.

The pressure amplitude of a spherical wave diverging from a point source in a perfectly elastic medium is inversely proportional to the travel distance (15, p. 167). As rock is never perfectly elastic, particularily at the level of stress encountered in blasting, the pressure amplitude in the rock will decrease more rapidly with increasing distance than in the case of a perfectly elastic medium. The pressure in the material at different travel distances is generally expressed as follows:

$$P_r = \frac{K}{x^{\beta}} \qquad (13)$$

The theoretical work of Sharpe (31) indicated that the above pressure-distance relationship is valid but that the absorption coefficient "β" will decrease with increasing travel distance. However, the variation of wave travel distances in rock blasting is small, so the absorption coefficient would not be expected to decrease substantially. In this respect, Pickett (27, p. 72) determined the value of the absorption coefficient for shale and limestone to vary from 1.6 to 3.4, with an average value of 2.2. The value for the constant K was between 2.4×10^6 and 22×10^6. Duval (9, p. 315) found that the magnitude of the absorption coefficient ranged from 1.6 to 2.5 for various rock types and explosives. A slightly different expression had been proposed by Hino (12, p. 31)

for the rock pressure at increasing travel distances:

$$P_r = P_d \left(\frac{a}{x}\right)^{\beta} \qquad (14)$$

For a solution it would not be necessary to experimentally determine the constant K, simplifying calculations. The absorption constant determined by Hino was found to be 1.8 when 40% du Pont Gelex was detonated in granite. However, the detonation pressure of the explosive must be determined in order to utilize the expression.

Effect of Single Free Face-Point Charge

The introduction of a free face or a density discontinuity disrupts passage of a compressive wave. Upon coming in contact with a discontinuity a portion of the original energy of the compressive wave is reflected back into the original material, while part of the energy is refracted into the second medium. The ratio of the intensity of the initial wave to that of the reflected wave depends on the characteristic impedence difference of the two materials and on the angle of incidence of the impinging compressive wave (15, p. 147).

The characteristic impedence of a material is defined as the ratio of the pressure in the medium to the associated particle velocity (15, p. 135). For plane waves the characteristic impedance is a constant,

$$Z = \rho V_e \qquad (15)$$

while in the case of spherically diverging waves it becomes a function of the travel distance, as follows:

$$Z = \rho V e^{\frac{Wx}{(1+W^2x^2)^{\frac{1}{2}}}} \qquad (16)$$

In rock blasting the usual free face is that between rock and air, in which case the characteristic impedance ratio is on the order of 10^5 to 1. Since the difference in the characteristic impedence of the two materials is so large, the ratio of the incident and the reflected pressures approaches minus one (15, p. 147), regardless of the angle of incidence. Thus, a coefficient of reflection for a rock to air boundary of minus one can be used as a first approximation. The minus sign in the ratio indicates that a tensile wave is produced by the reflection of a compressive wave at the free face.

The tensile wave travels back into the rock mass superimposing its particle motion onto that of the compressive wave. At a specific distance from the boundary the resultant tensile stress in the rock exceeds the tensile strength of the rock, and failure will result. The first slab formed will have imparted to it a velocity equal to twice the particle velocity of the entrapped tensile wave. Tensile slabbing will again occur if the tensile strength of the rock is again exceeded, forming another free face, so that the process continues to repeat itself until the reflected tensile pulse no longer exceeds the tensile strength of the rock. The number and thickness of slabs that are formed is dependent on the magnitude and shape of the initial stress pulse, and calculations have been developed for this determination by Hino

(12, p. 24). Figure 2 illustrates the steps involved in multiple slabbing.

Effect of Multiple Free Faces - Point Charge

Tensile waves formed by the reflection of an incident compressive wave from two or more free faces will collide in the rock, resulting in large localized tensile stresses (30). Very pronounced cracks will form by the interaction of these tensile waves, beginning at the corner of the rock and progressing back into the rock mass, as is shown by Figure 3. The direction of the crack produced by the interaction of the reflected waves formed by initiation of a point charge is a function of the respective travel distances of the various reflected waves. A study of the equations of the reflected wave surfaces shows that, as can be seen in Figure 3,

$$\text{Tan. } Q = \left(\frac{L}{B}\right)^{-1} \qquad (17)$$

For a vertical plane the angle of the fracture will be at 45 degrees when the vertical height of the bench (L) is equal to the horizontal burden (B) distance. A similar relationship exists for the horizontal plane when a charge is placed equidistant from two perpendicular vertical free faces. The development of this fracture along the intersection of two vertical free faces is also shown in Plate 7, (see Appendix D).

If the slabbing process from one free face reaches the charge position before that from the other free face,

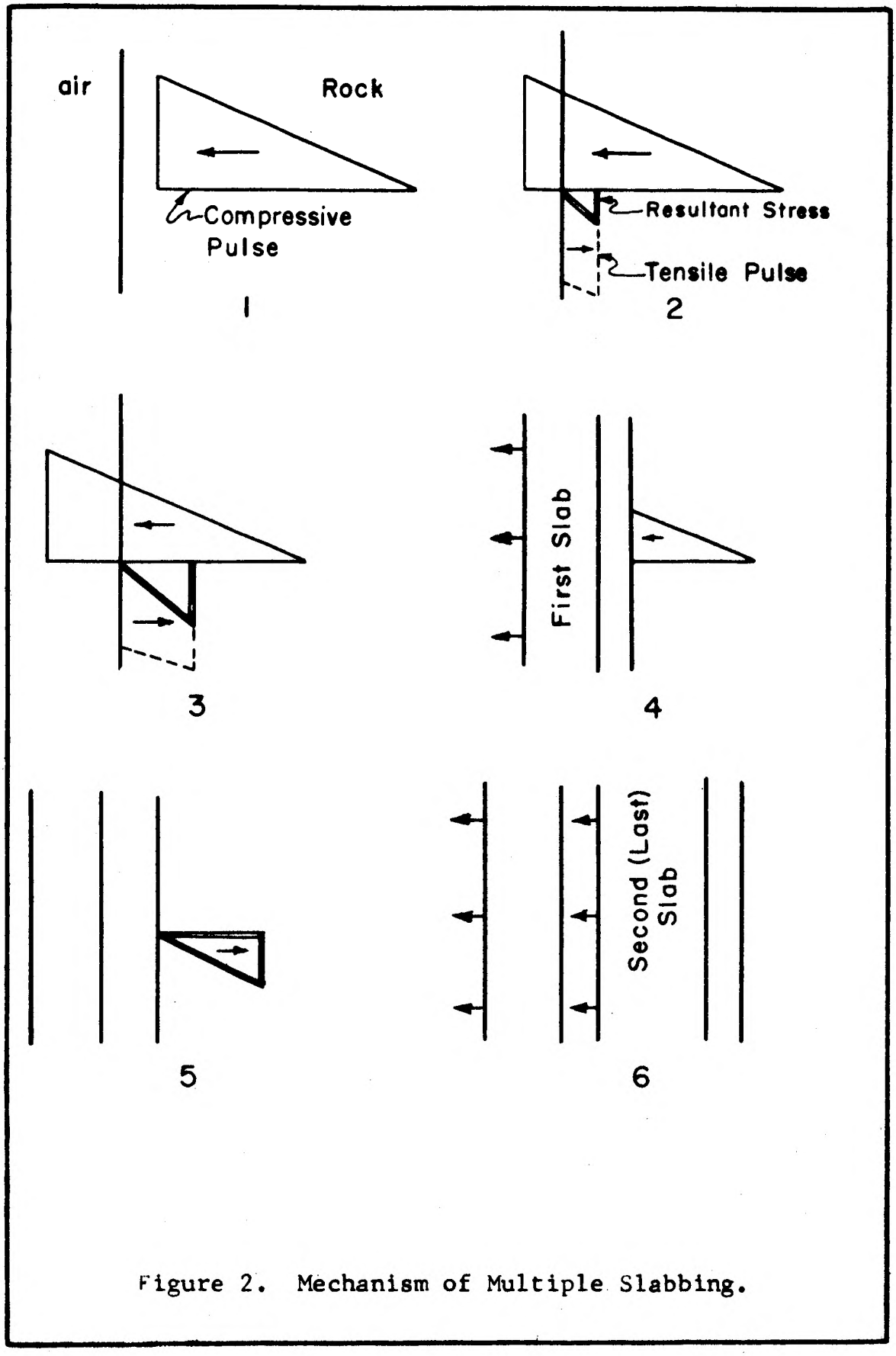

Figure 2. Mechanism of Multiple Slabbing.

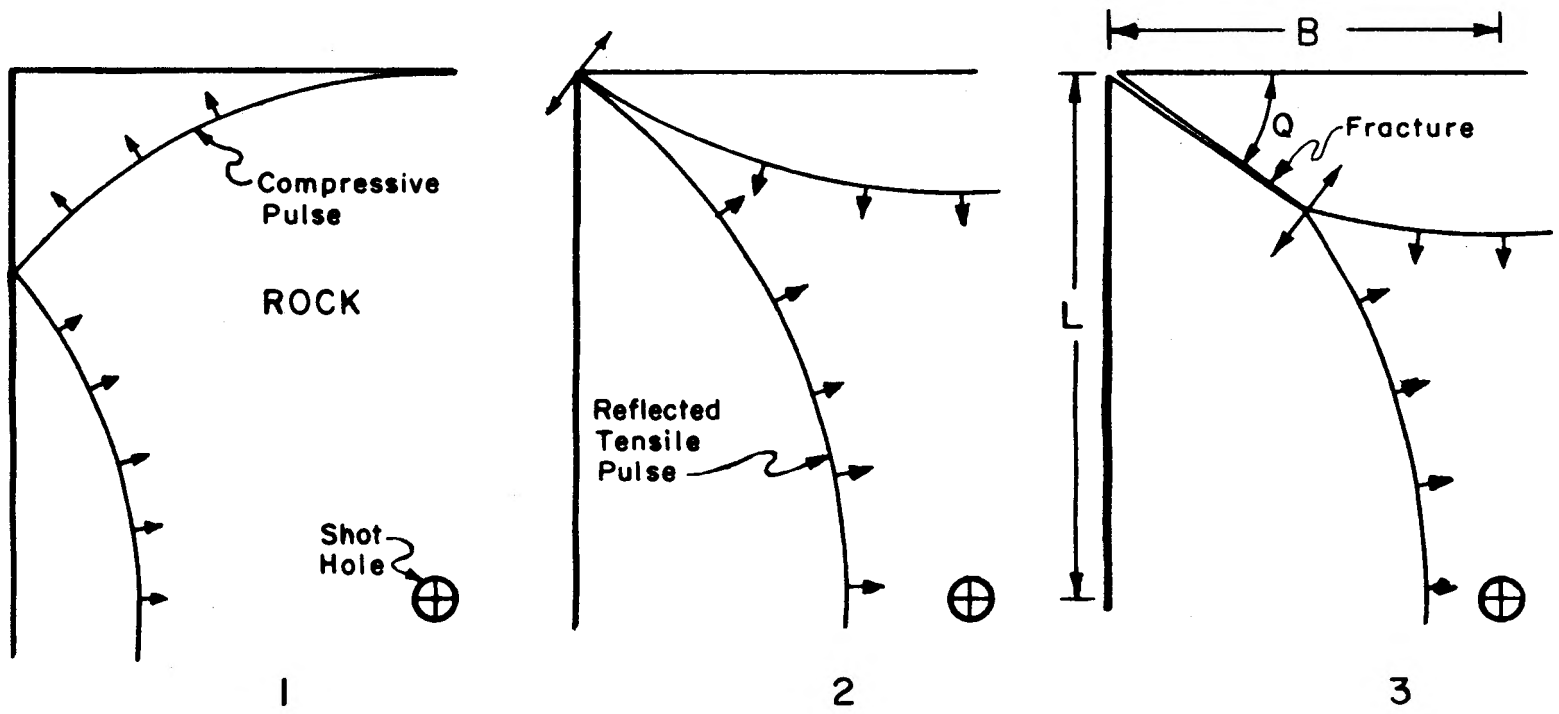

Figure 3. Fracture Formation by Interaction of Tensile Waves.

the gases will be relieved in the direction of the first free face, Once the gases have escaped from the charge-hole no further pressure can be exerted on the rock. The slabbing action ceases when the pressure in the borehole is relieved. Unless the reflected pulses from all free faces arrive back at the borehole at the same time non-uniform fragmentation will result.

Cratering will always occur in the direction of relief taken by the detonation products. Thus, the vertical height to horizontal burden ratio for a point charge in a bench blast must be equal to one to prevent the formation of non-uniform stressing, which could result in boulders or overbreak, or both.

Effect of Multiple Free Faces - Cylindrical Charge

In order for the geometry of point charge to be balanced to give uniformily broken rock, the arrival time of the compressive wave at all free faces must be equal. It would be expected that the same principle would hold true when a cylindrical charge is employed. The rock must be stressed in a uniform manner if maximum beneficial utilization of the explosive energy is to be attained. Thus, when using a cylindrical explosive charge the detonation velocity of the explosive itself, in respect to the rock's longitudinal wave velocity, would become a very important parameter.

The shape of the wave front in the rock that results from the initiation of a column of explosive depends

largely on the explosive reaction rate. If the explosive velocity is greater than the longitudinal wave velocity of the surrounding rock, the resulting wave front will be shaped as a truncated cone. The angle of the cone around the borehole can be determined as follows (28,p62):

$$\text{Sin } \theta = \frac{V_r}{V_e} \tag{18}$$

If the explosive velocity is equal to or less than the wave velocity of the rock, the resulting wave front will be spherical. The only difference between the two is in the distribution of the pressure amplitudes along the wave front. Figure 4 illustrates three different cases.

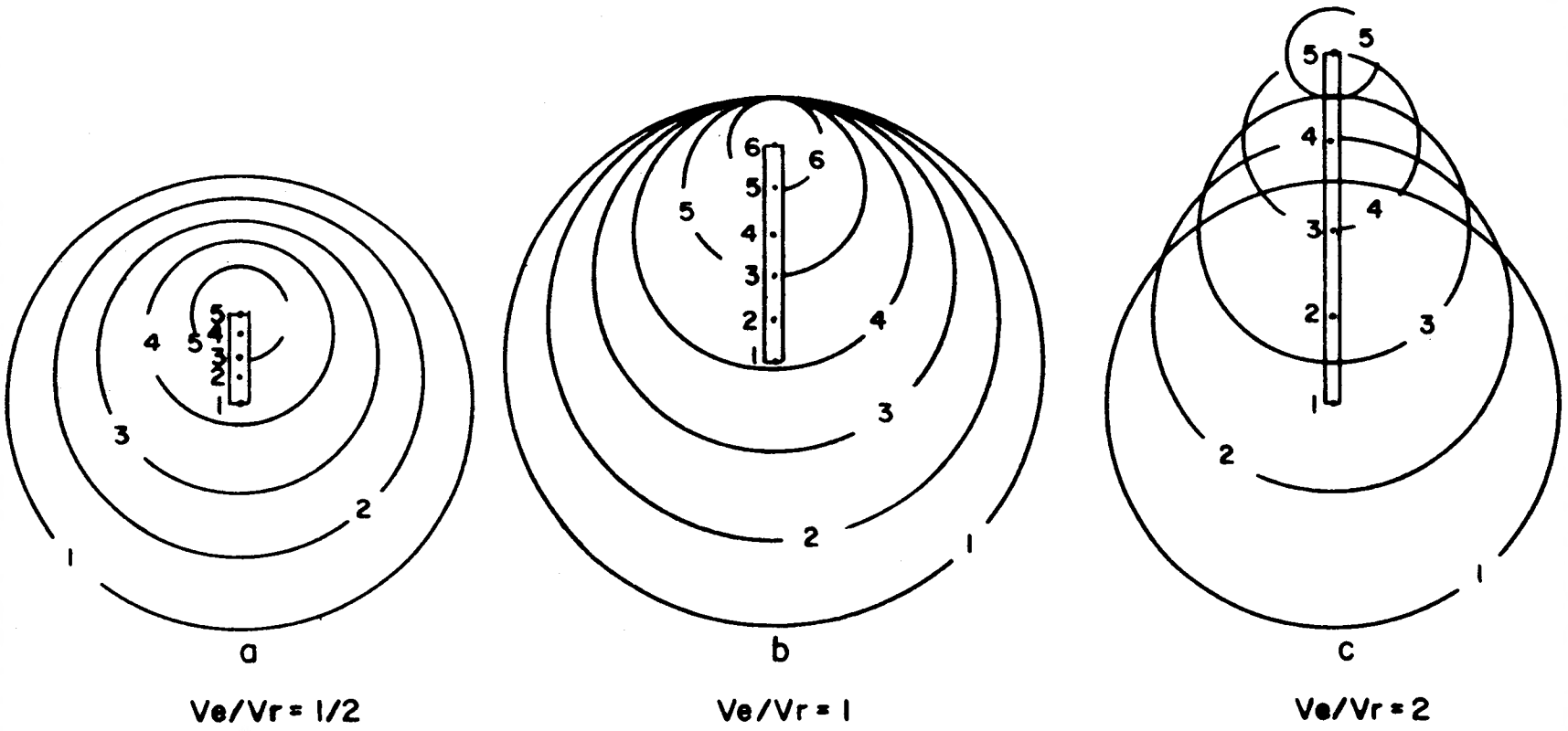

Figure 4. Distribution of Pressure Wave Fronts in Rock (Bottom Primed).

CHAPTER III

INFLUENCE OF CHARGE LENGTH AND VELOCITY RATIO ON BLAST DIMENSIONING

When blasting with cylindrical charges, the individual blasting mechanisms such as tensile slabbing will occur as that described for blasting with point charges. However, the introduction of a cylindrical charge alters the relative importance of each in terms of the overall blasting process. The rate of energy propagation through the explosive and through the rock, when different, will modify the state of stress that is generated in the rock.

The Dependency of Detonation Pressure on Density and Velocity

It has been shown that the magnitude of the stresses produced in the rock from an explosive is dependent on the pressure developed during detonation. The detonation pressure of a large number of commercial explosives has been calculated by Hino (12) using Equation 11, the coefficients of which were determined by H. Jones. This equation related the detonation pressure of an explosive to the explosive detonation velocity and density. In Figures 5, 6, and 7 different combinations of the three explosive parameters are related graphically. From Figure 5 it can be observed that for commercial explosives there appears to be no distinct relationship between explosive density and explosive detonation pressure. This would be expected

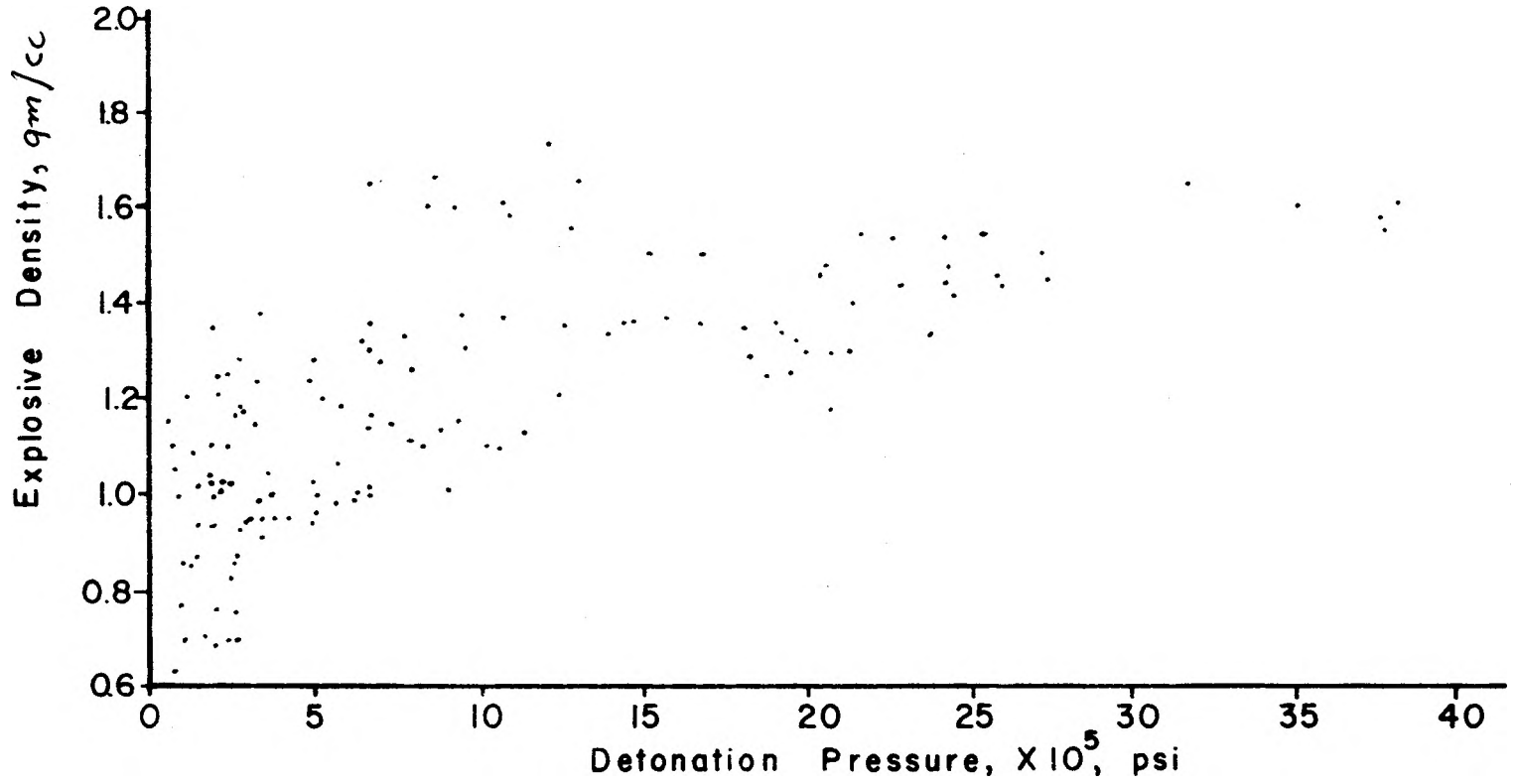

Figure 5. Density - Detonation Pressure Relationshipe for Commercial Explosives.

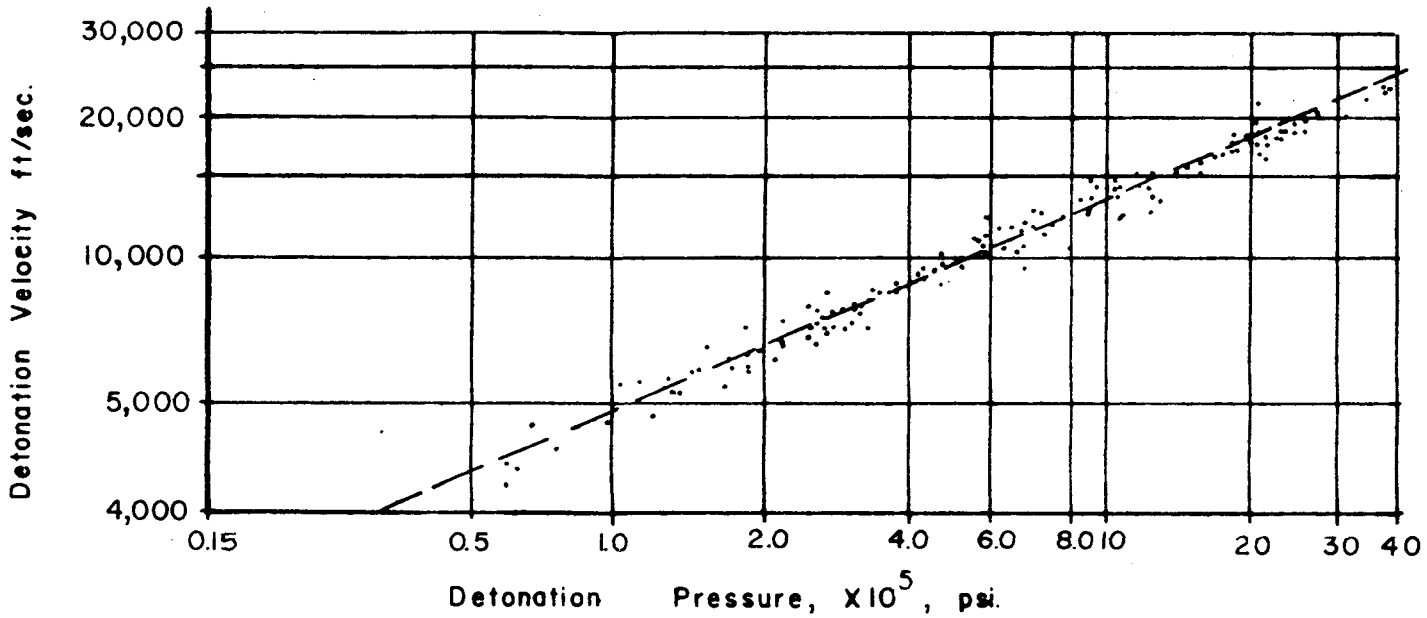

Figure 6. Velocity - Detonation Pressure Relationships for Commercial Explosives.

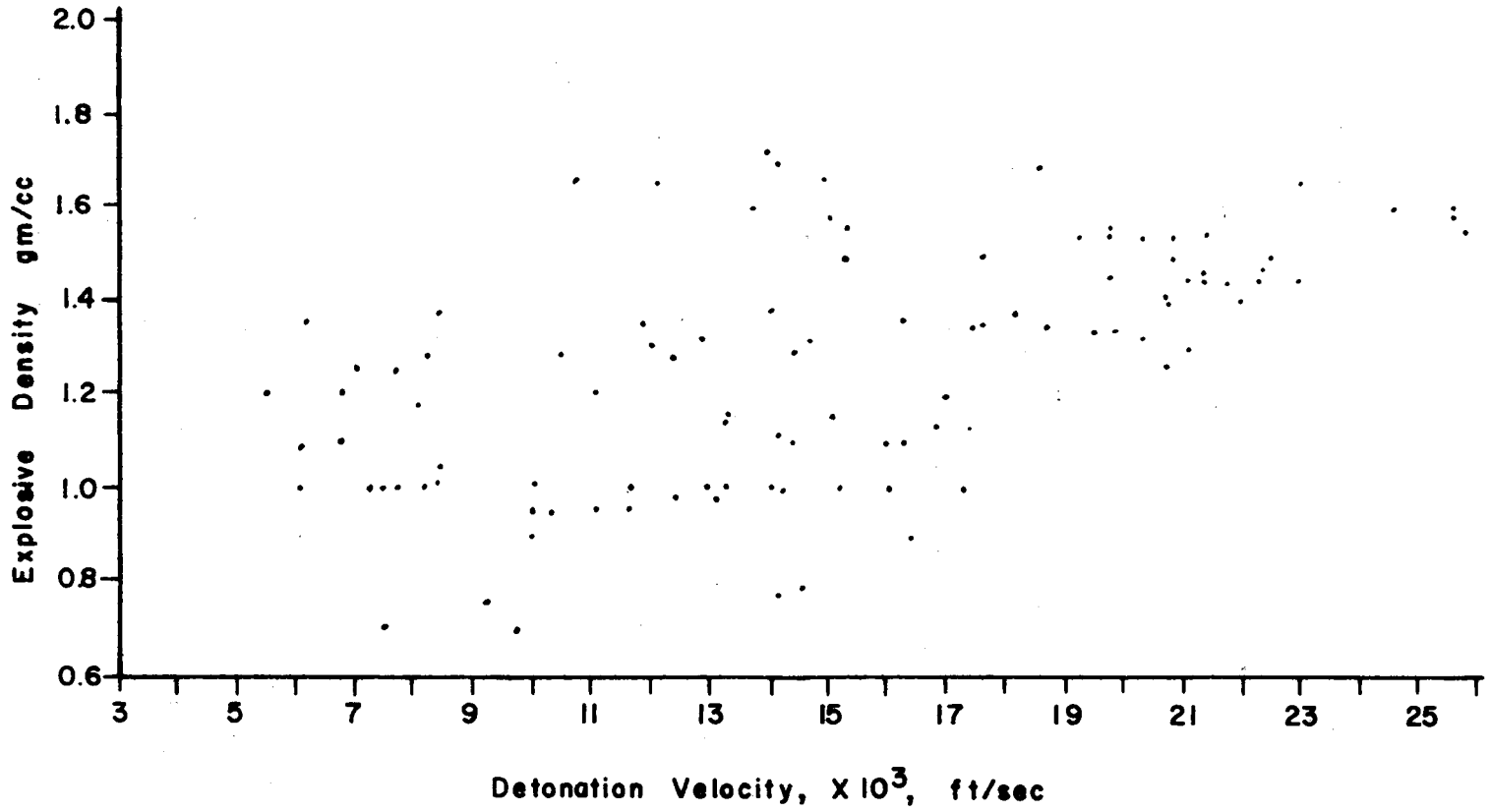

Figure 7. Velocity - Density Relationships for Commercial Explosives.

since various nonreactive additives are often included in the composition of commercial explosives to give certain specific characteristics for particular blasting applications. The explosive density, therefore, can be considerably altered from the ideal by the addition of inert or low order ingredients whose density is much different than that of the included explosive compound. Figure 6 shows the relationship between detonation velocity and detonation pressure for many commercial explosives. As can be seen the relationship when plotted on a log-log scale is nearly linear. It is suggested then, that the detonation velocity should be used as the preferred index for detonation pressure. The equation for the relationship shown by Figure 6, relating the detonation pressure to the reaction velocity, is as follows:

$$P_d = 3.285 \times 10^{-4} (V_e)^{2.28} \qquad (19)$$

where: P_d is in pounds per square inch,

V_e is in feet per second.

Figure 7 illustrates the relationship between the explosive density and the detonation velocity for many commercial explosives. There appears to be no distinct relationship for converting one to the other.

Influence of Initiator Position

It has been shown that the explosive detonation velocity largely determines the detonation pressure of an

explosive and that it strongly influences the shape of the wave front in the rock. Another factor that would control blasting effects is the position of the primer in an explosive column and the direction of initiation. The two most commonly used primer locations in practice are collar priming and bottom priming.

To avoid stress unbalance and prevent a premature loss of energy the pressure wave in the rock should reach the vertical and the horizontal free face at the same instant, or it must reach the base of the vertical free face first. This is because the bottom of a bench (floor level) offers the most resistance to breakage and movement.

Bottom Priming

When an explosive charge is initiated at the bottom, it is desired that the pressure wave in the rock reach the base of the vertical free face either before, or at the same time as it reaches the horizontal free face at the bench top. If this condition, herein termed time-stress balancing, is to be satisfied, the bench height must equal or exceed the horizontal burden dimension. Therefore, a minimum height-to-burden ratio must exist. If the height-to-burden ratio is less than this minimum, the pressure wave will reach the horizontal free face at the bench top first. Cratering from premature stressing at the collar would then be expected to occur.

An expression for the minimum height-to-burden ratio

for bench blasts having two mutually perpendicular free faces has been derived (see the Appendix). Charge length, charge initiation position, and the velocity of the explosive detonation wave and that of the shock wave through the medium to be blasted are considered. For bottom priming the relationship is as follows:

$$\frac{L}{B} = \frac{T}{B}\left(1 - \frac{V_e}{V_r}\right) + \frac{V_e}{V_r}\left(1 + \left[\frac{J}{B}\right]^2\right)^{\frac{1}{2}} - \frac{J}{B} \qquad (20)$$

The minimum height-to-burden ratios (L/B), for various stemming ratios (T/B) and subdrilling ratios (J/B), are plotted against the velocity ratio (Ve/Vr) as shown in Figure 8. Figure 18 illustrates the terminology. An analysis of the minimum L/B equation and Figure 8 indicates that the several following relationships would exist for bottom primed cylindrical charges:

1. The minimum L/B value increases with an increasing Ve/Vr ratio, when T/B $\leq$ L/B.
2. The minimum L/B ratio decreases for a constant Ve/Vr value for an increasing T/B.
3. The minimum L/B value is a constant, regardless of T/B when Ve/Vr equals 1 at specific values of J/B.
4. The minimum L/B ratio decreases as J/B increases, for any set of values of Ve/Vr and T/B.
5. The slope of the minimum L/B vs. Ve/Vr curve increases as J/B increases, and decreases as T/B increases.

Careful consideration of the practical meaning of the relationships indicated by Equation 20 reveals that several limitations must be applied. The subdrilling ratio, as

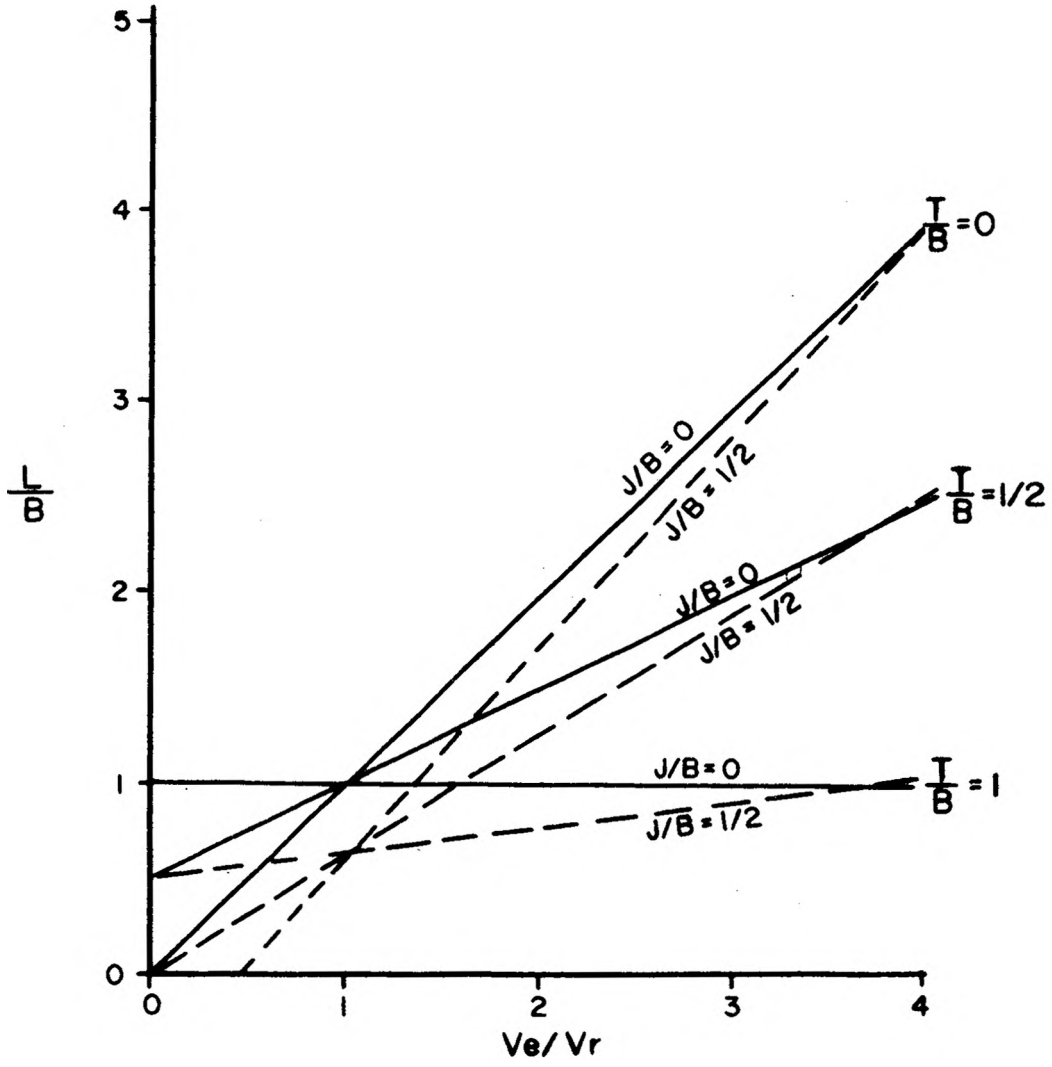

Figure 8. Minimum L/B Ratio for Bottom Priming.

well as the stemming ratio, is controlled by the characteristics of the rock being blasted. The exact amount of these two parameters cannot be determined simply by using Equation 20. However, L/B must always be greater than T/B when J/B equals zero, i.e., $L/B \rangle T/B$ for $J/B = 0$. Otherwise, the amount of stemming that is necessary to balance the shot should equal or exceed the total hole depth. The expression shows that the maximum T/B value that can be employed would be one, a situation that is analogous to the use of a point charge when L/B equals one.

The effect of J/B on the minimum L/B depends on Ve/Vr. The slope of the relationship for the minimum L/B vs. Ve/Vr, at any specific T/B value, increases as J/B increases. The point of intersection of the line with the vertical axis decreases with increasing J/B.

When Ve/Vr is less than one, the minimum L/B value, as predicted by Equation 20, becomes less than one. However, in this instance the rate of travel of the pressure wave in the rock leads the detonation wave in the explosive, as is shown by Figure 4a. Pressure waves from the bottom of the explosive charge, i.e., from the point of initiation, will reach the horizontal surface first, introducing immediate tensile slabbing and cratering at that face. The pressure waves from the ascending detonation wave of the charge will continously impinge with increasing intensity on the horizontal surface that is already under tensile stress. The resisting vertical

burden on the upper portion of the charge will be rapidly decreased and a violent blast will occur with damaging overbreak. This mechanism explains observed effects from low velocity explosives when used in rock having a higher longitudinal wave velocity. To prevent violence and overbreak the L/B value must then never be less than one. Therefore, practical limits for using Equation 20 would be when Ve/Vr is equal to or greater than one. Plate 8, in Appendix D, shows the sequence of breakage of a bottom primed, well balanced blast.

Collar Primed

As for bottom priming, the pressure wave from an explosive charge initiated at the collar, or top, should reach the base of the vertical free face earlier than, or at least at the same time, it reaches the horizontal free face to insure balanced stressing. The time required for it to reach the horizontal free face would be constant for a fixed amount of stemming. The time required for the pressure pulse to reach the base of the vertical free face will increase as the bench height increases for a constant burden dimension and stemming ratio. Thus, a maximum L/B ratio must exist for collar priming. If L/B increases beyond the maximum value, air blast, flyrock and overbreak, coupled with toe formation at the base of the ledge could result.

An expression for the maximum L/B ratio to insure

balanced stressing for collar priming has been derived from considerations similar to those for bottom priming (see Appendix B). The relationship follows:

$$\frac{L}{B} = \frac{T}{B}\left[1 + \frac{V_e}{V_r}\right] - \frac{V_e}{V_r}\left[1 + \left(\frac{J}{B}\right)^2\right]^{\frac{1}{2}} - \frac{J}{B} \qquad (21)$$

This equation is similar, except for a change in the signs, to that obtained for determining the minimum L/B ratio for bottom priming. An analysis of the physical meaning of Equation 21 reveals pronounced differences between the two priming locations as to the blasting techniques that must be employed.

The relationships that exist for collar priming are summarized below:

1. The maximum L/B ratio increases as Ve/Vr increases, at specific T/B and J/B ratios.
2. The maximum L/B ratio increases as T/B increases, and decreases as J/B increases, for a given Ve/Vr.
3. The slope of the maximum L/B ratio for each specific Ve/Vr value decreases as J/B increases for a constant T/B ratio.

The features of Equation 21 are illustrated by Figure 9.

Definite practical limits exist for the maximum L/B ratio equation, which can be determined by considering the practical limits for a blast design. The stemming ratio, as is the case of bottom priming, should never exceed L/B when J/B = 0. Thus, that portion of Figure 9 which indicates a L/B ratio less than the stemming ratio should not be used for design purposes.

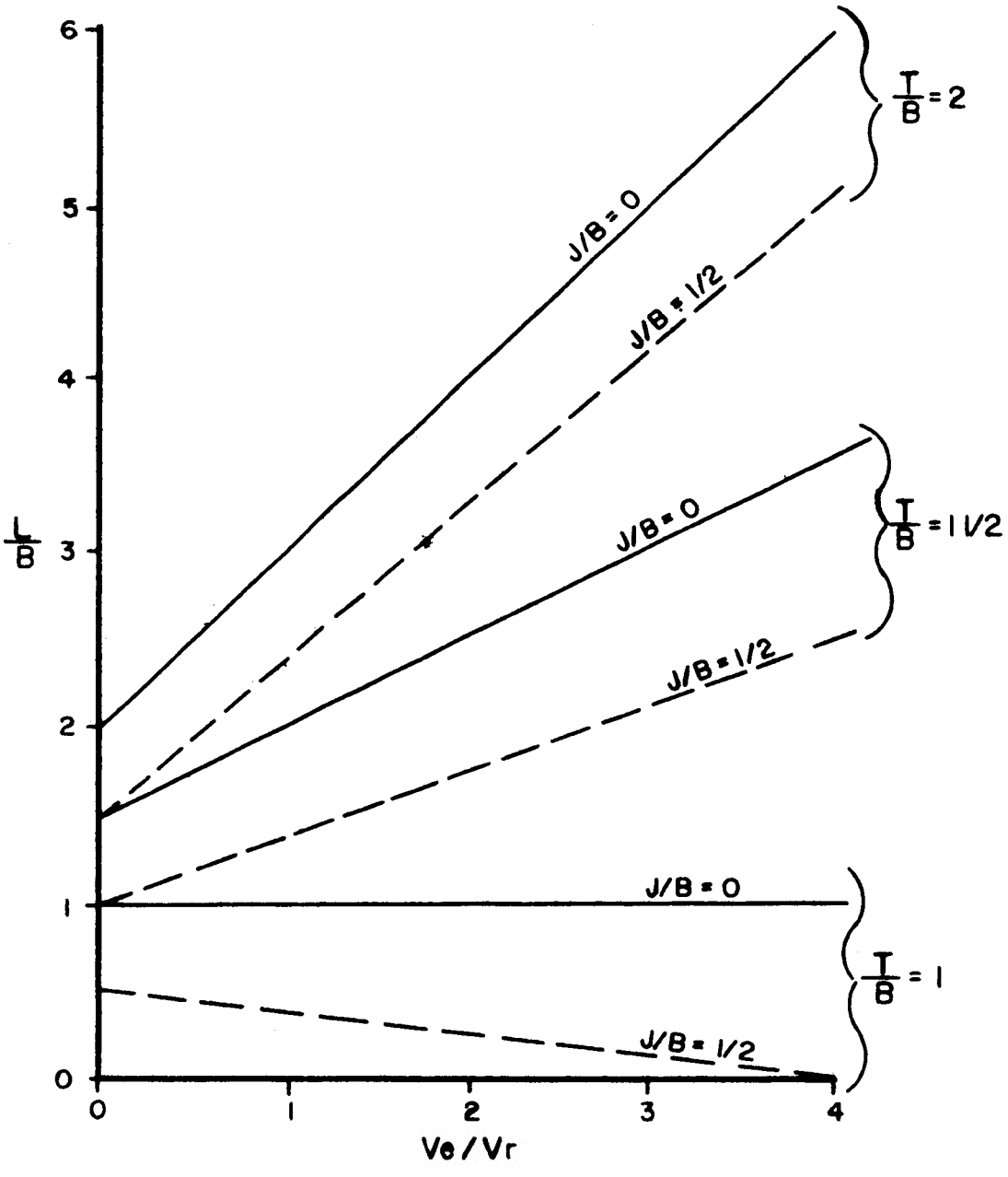

Figure 9. Maximum L/B Ratio for Collar Priming.

As J/B increases for a constant T/B ratio, the maximum L/B ratio decreases until it is the same as T/B. This point marks the lower limit for the L/B value.

If T/B is less than one for collar priming, the maximum L/B ratio would always be either zero or negative in value. This means that for this situation it is impossible for the pressure wave to reach the base of the vertical free face before or at the same time it reaches the horizontal free face. Thus, T/B should be greater than one. However, when T/B becomes greater than one, insufficient energy is imparted to the rock at the top of the bench for adequate fracturing and large slabs are likely to form in this area. If T/B is less than one, the blast will again be unbalanced, with the inevitable result being top cratering. Air blast, overbreak, and flyrock could be expected. Plate 9 shows the breakage sequence of a blast that was collar primed (Appendix D).

Effect of Charge Length on Stress Distribution

In most investigations on blast design the explosive charge has been assumed to be concentrated at a single point. The nature of the stresses in the rock generated by a diverging pressure pulse has been discussed in CHAPTER II. When a cylindrical charge is employed, however, the stresses in the rock resulting from detonation at different points along the explosive charge will interact

with one another. The interaction of different stress pulses in the rock will result in a total stress distribution that would be expected to differ from that of a point charge. Both the direction and magnitude of the forces at different points in the rock will be affected. Thus, a blast must be designed so that the magnitude and direction of the forces at different points in the rock will be such that maximum utilization of the energy can be attained (2, p. 311).

By studying the stress distribution in rock around a cylindrical charge it can be seen that the distribution is largely dependent on the velocity ratio. The resultant stress at any point in the rock is equal to the vector sum of the stresses generated from each point along the charge length. The energy level at any point in the rock is dependent on the position of the point and the rate that energy flows through that point. The rate at which energy is delivered to a point is dependent on the detonation pressure of the explosive and the energy propagation rate of the rock, while the rate of energy transfer away from the rock is dependent solely on the energy propagation rate of the rock. Thus, the explosive velocity and the rock energy propagation characteristics largely determine the state of stress at any particular point in the rock.

A graphical method of analysis provides a convenient method for investigating the changes in the total force at

any point in the rock. The method used for this investigation considers, by resolution, the individual forces from different points along the charge length and the tensile force along the reflected wave front. The total resultant force in the rock at any point can then be determined. The pulse length is considered to be equal to twice the burden dimension, while its shape is assumed to be triangular. The decay of the pressure in the rock due to divergence of the wave and energy losses by absorption is assumed to be proportional to the inverse square of the travel distance. It is also assumed that there is perfect force-coupling between the explosive and the rock. Since tensile breakage will occur along the reflected wave front the analysis is restricted to the variations of the total force at different points along this front.

The analysis shows that the magnitude and direction of the total force at a given time is dependent on the position of the point in the rock, the charge length, and the velocity ratio. Figures 10, 11, and 12 show the direction and relative magnitude of the total force along the reflected wave front for different velocity ratios when the explosive charge is bottom primed and there is no subdrilling. The important feature that should be noted is that the direction of the total force varies from horizontal at the free face to nearly vertically downward at the base of the blast-hole. This indicates

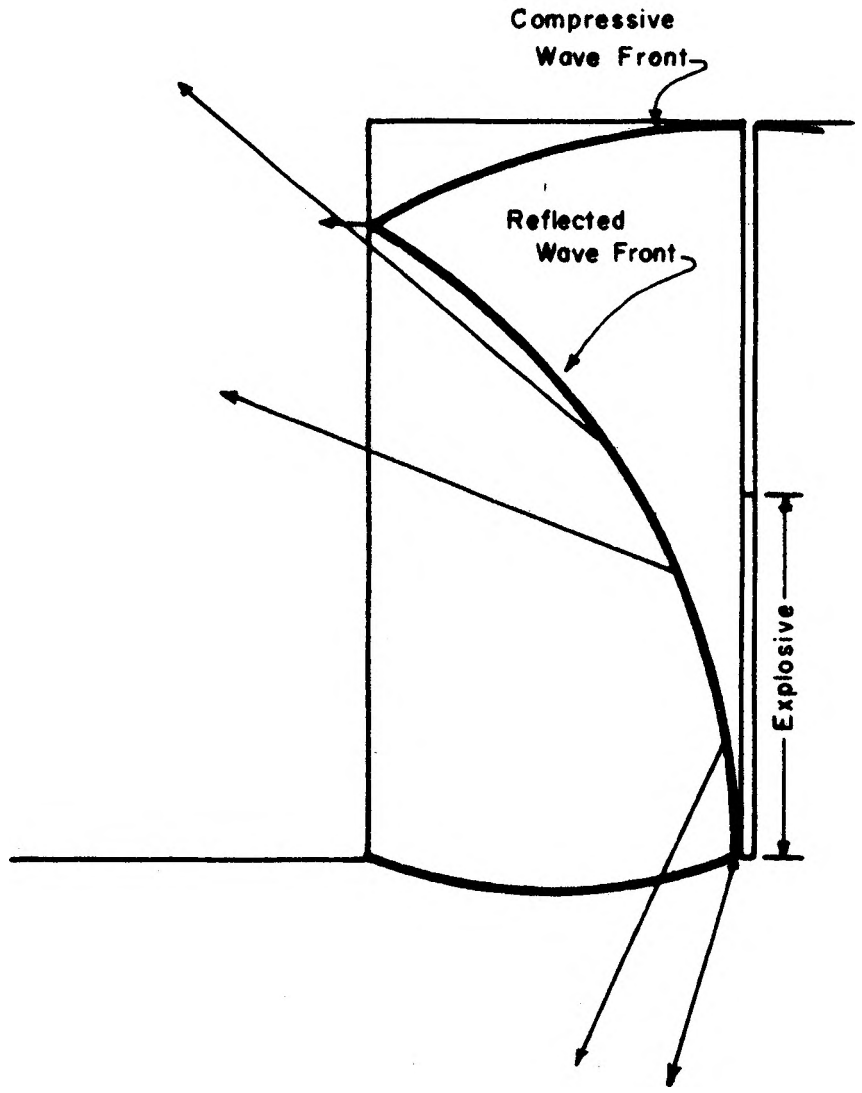

Figure 10. Force Distribution Along Reflected Wave Front, for Vc/Vr = ½.

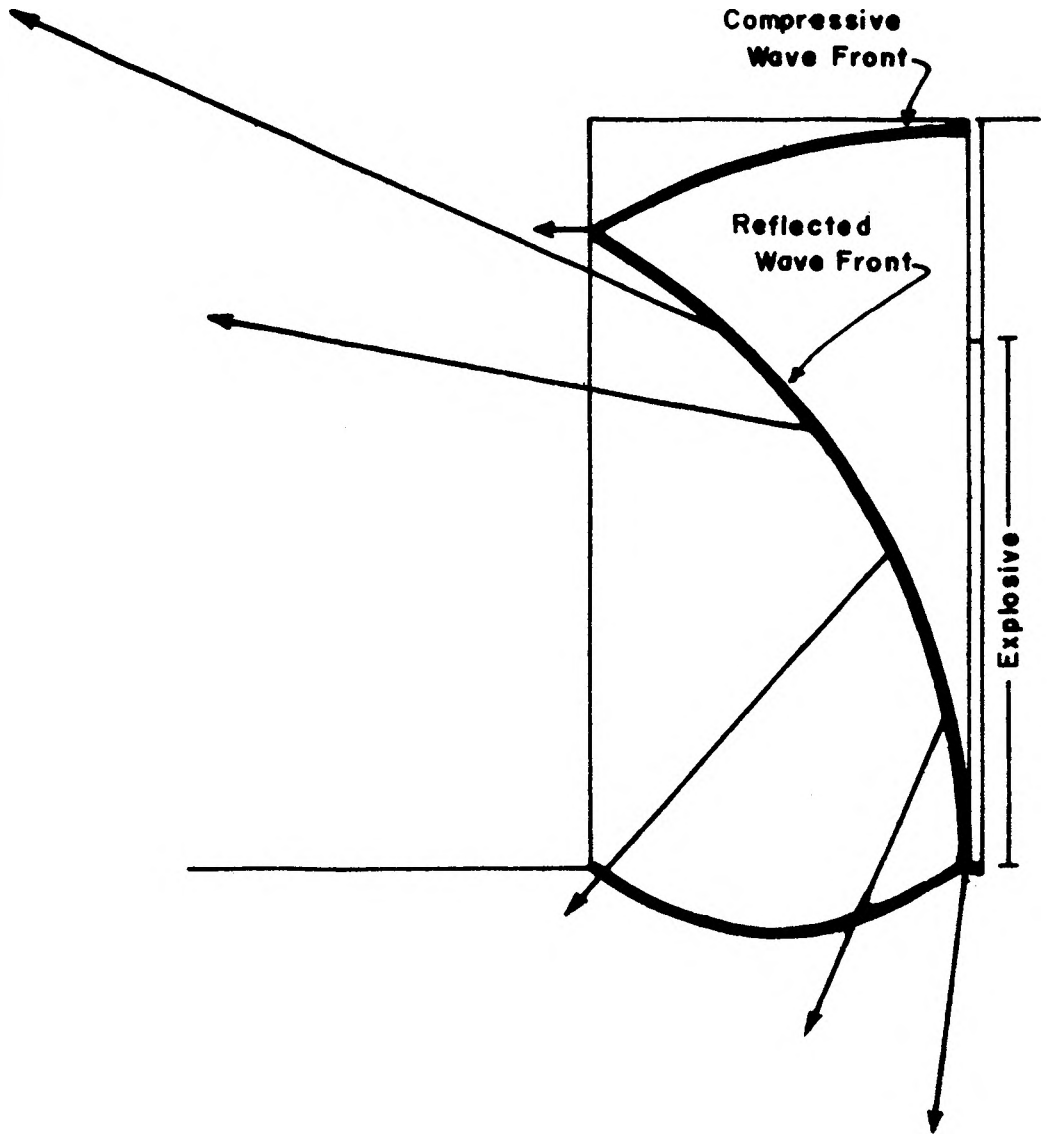

Figure 11. Force Distribution Along Reflected Wave Front, for Ve/Vr = 1.

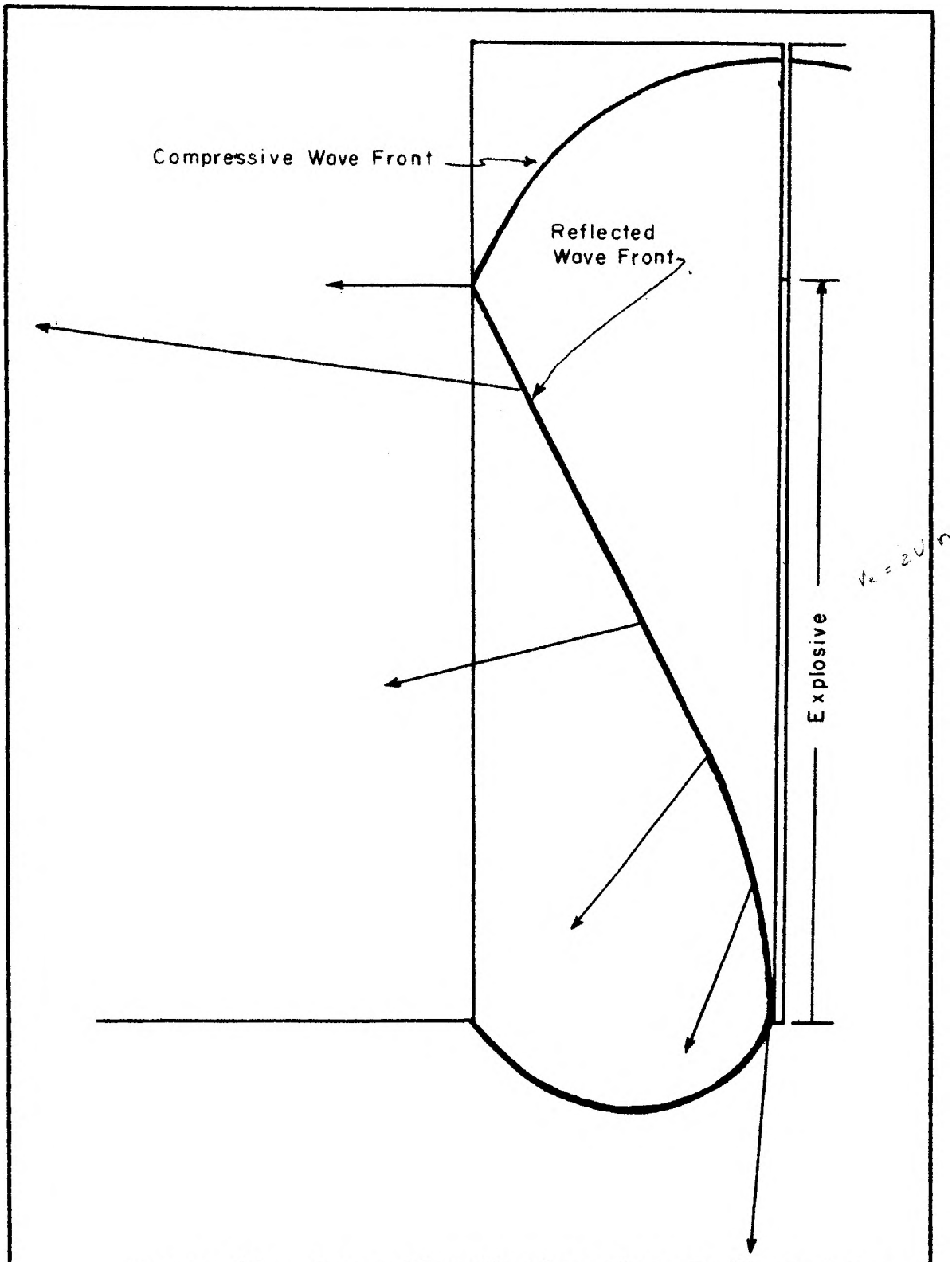

Figure 12. Force Distribution Along Reflected Wave Front, for Ve/Vr = 2.

that rock breakage by tension at the base of the blast-hole would be unlikely, since the tensile wave cannot cause rock breakage unless the overall stress is tensional along the wave front and is directed so that movement of the rock is not prevented. As the velocity ratio increases, the forces at the base of the bench become even more steeply inclined. This is to be expected since at any one instant a greater portion of the total energy of the charge would have been imparted into the rock when using higher velocity explosives.

To prevent the formation of a toe, or bootleg, the horizontal component of the total tensile stress at the base of the bench must exceed the tensile strength of the rock. It appears, however, that in the absence of subdrilling the predominant direction of the stresses in this area is nearly vertically downward. The direction of the total force along the reflected wave front at the base of the bench is horizontal at the free face but becomes inclined downward as the wave front proceeds back into the rock. At a specific distance from the free face the horizontal component of the tensile stress becomes too weak to cause breakage, and a toe will then begin to form. This effect has been noted from field observations, where the toe formed is located nearest the blast-hole, not at the outside portion of the burden. Subdrilling, therefore, serves to increase the magnitude of the horizontally directed component of stress at the base of the ledge.

The resisting burden on the explosive in the upper portion of a cylindrical charge is much less than the initial burden dimension, since tensile stressing has broken much of the rock at the base of the bench before the pressure pulse from the upper portion of the charge has had time to act. Thus, the slab velocity of the rock broken from those areas where the burden has been reduced would be expected to be greater than that of the slabs broken first. Petkof (26) found experimentally that the velocity of the first formed slabs increases in a stepwise fashion. The slabs formed nearest the blast-hole would have a greater velocity than those formed from the original free face, which would then collide with the latter causing a stepwise increase in their velocity.

CHAPTER IV

FIELD BLASTING TECHNIQUES

The effect of rock discontinuities such as jointing and stratification planes was not considered in the theoretical analysis. It should be understood, however, that the theoretical conclusions must be modified for blasting under actual field conditions. In order to substantiate the theoretical work the following two separate studies were conducted: 1. A series of test blasts were made to determine the influence of geologic structure and effect of two mutually perpendicular free faces on blast results, and 2. An intensive study was made of many field blasting practices so that a correlation could be made between the theoretical work and actual field techniques.

Experimental Investigation

Two blasts were made at the Missouri School of Mines Experimental Quarry. The blasts were designed to investigate the blast effects that might occur when using different L/B ratios. The influence of structural planes of weakness, such as joints, seams, and stratification planes, was noted.

The rock at the school quarry is a soft, nearly horizontal dolomite of the Jefferson formation, characterized by pronounced stratification planes and vertical joints.

The physical properties of the rock were reported by Yancik (33, p. 5).

The diameter of the blast-holes for both test blasts was 1½ inches, and in both cases the explosive used was Atlas 60% Extra Dynamite in 1¼ X 8 inch cartridges. The blasts were intentionally underloaded so that complete rock breakage and ejection would not occur. In this manner it would be possible to observe the nature and distribution of the cracks and tensile slabs formed.

Figure 13 shows the details of Test Blast Number 1, where L/B = 1, T/B = 0.875, J/B = 0, and Ve/Vr = 1.05. According to theoretical considerations, this blast should produce uniform stressing in the rock, and the degree of cratering at both free faces should be the same. Plates 1 and 2 illustrate the blast site before and after intiation of the blast, while Plate 3 is a close-up photograph of the cracks that were formed on the horizontal free face. Several important features are shown by the photographs. Two pronounced horizontal bedding planes and vertical joints are evident on the vertical free face. Since the amount of explosive energy for the blast was low, little cratering action could be expected at either free face. As can be seen from the photographs, no cratering was visible on the horizontal free face, indicating a balanced stress distribution throughout the rock. Small amounts of tensile slabbing occurred on the vertical free face

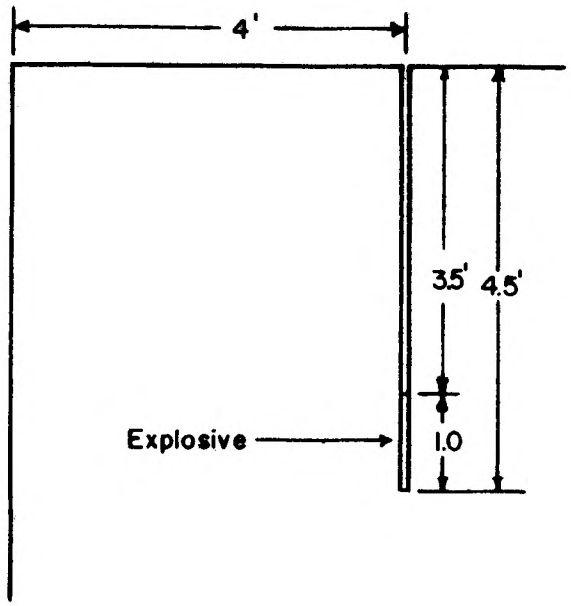

Figure 13. Design Details of Test Number 1.

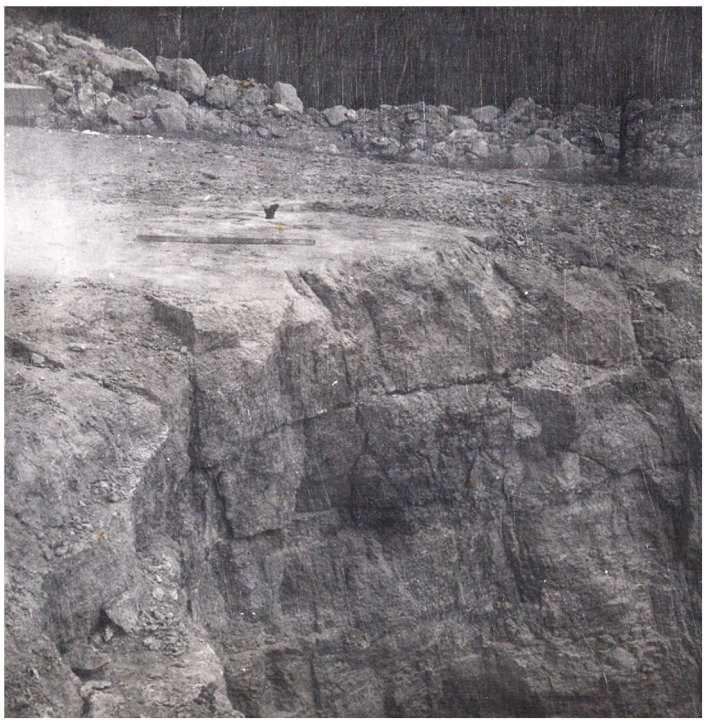

Plate 1. Test Number 1 Before Blasting.

Plate 2. Test Number 1 After Blasting.

Plate 3. Fractures Formed by Test Number 1.

directly below the two stratification planes, being the result of the interaction of tensile stress waves that were reflected from the vertical free face and the horizontal stratification planes. The stemming material was not ejected from the blast-hole by the explosive, indicating that the gaseous pressure was probably relieved along the stratification planes. It can be noted by Plate 3 that the cracks formed on the horizontal free face were parallel to the jointing pattern of the rock.

The L/B ratio for Test Number 2 was 0.667, as shown in Figure 14 and Plate 4, with all other conditions being the same as for the first blast. Cratering could be expected to occur at the horizontal free face, while only a minor amount would be expected on the vertical free face. The results of this blast are shown by Plates 5 and 6. As can be seen, pronounced cratering occured at the horizontal free face while there was a complete lack of tensile breakage on the vertical free face. Thus, the unbalanced state of stress that existed in the rock resulted in premature stress relief in the direction of the horizontal free face. Since the direction of relief was parallel to the blast-hole the explosive action expelled the stemming material (wet sand). The majority of the cracks formed were parallel to the jointing pattern in the rock as before.

The two experiments showed the importance of the positioning of free faces in controlling the resultant blast effects. When L/B is less than one, cratering can be

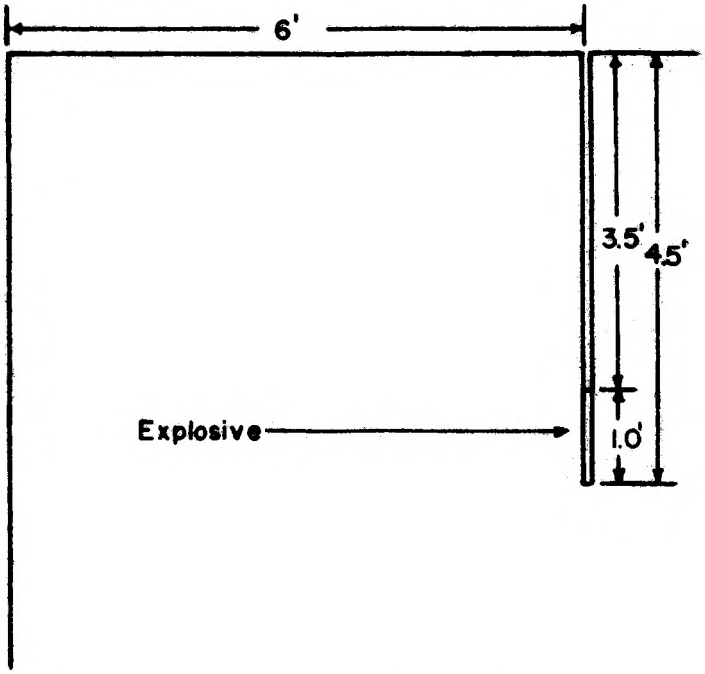

Figure 14. Design Details of Test Number 2.

Plate 4. Test Number 2 Before Blasting.

Plate 5. Test Number 2 After Blasting.

Plate 6. Crater Formed in Horizontal Free Face From Test Number 2.

expected at the horizontal free face. When L/B exceeds one, and T/B is larger than one, cratering can be expected to occur at the vertical free face. The results clearly substantiated theroetical predictions.

Correlative Survey of Blasting Practices

A study was made of field blasting practices, when vertical cylindrical blast-holes are used, so that actual field techniques could be determined. All types of operations except coal strippings were studied. The latter were omitted because of their unusual conditions. Information was obtained from many technical periodicals, a publication of the American Cyanimid Company, and data accumulated by Professor R. L. Ash of the Missouri School of Mines. The blast specifications reported in publications were most likely for blasts that were considered as successful.

The theoretical conclusions derived from this investigation involved both the stemming and subdrilling ratio; although a quantitative determination of these ratios was not undertaken. However, a determination of typical values used in industry would be of value. The mean, mode and median values for the two ratios were determined by standard statistical methods.

Figure 15 shows the frequency of usage of different stemming ratios, with 0.652 being the value of the mode, or that most commonly used in industry. The arithmetic

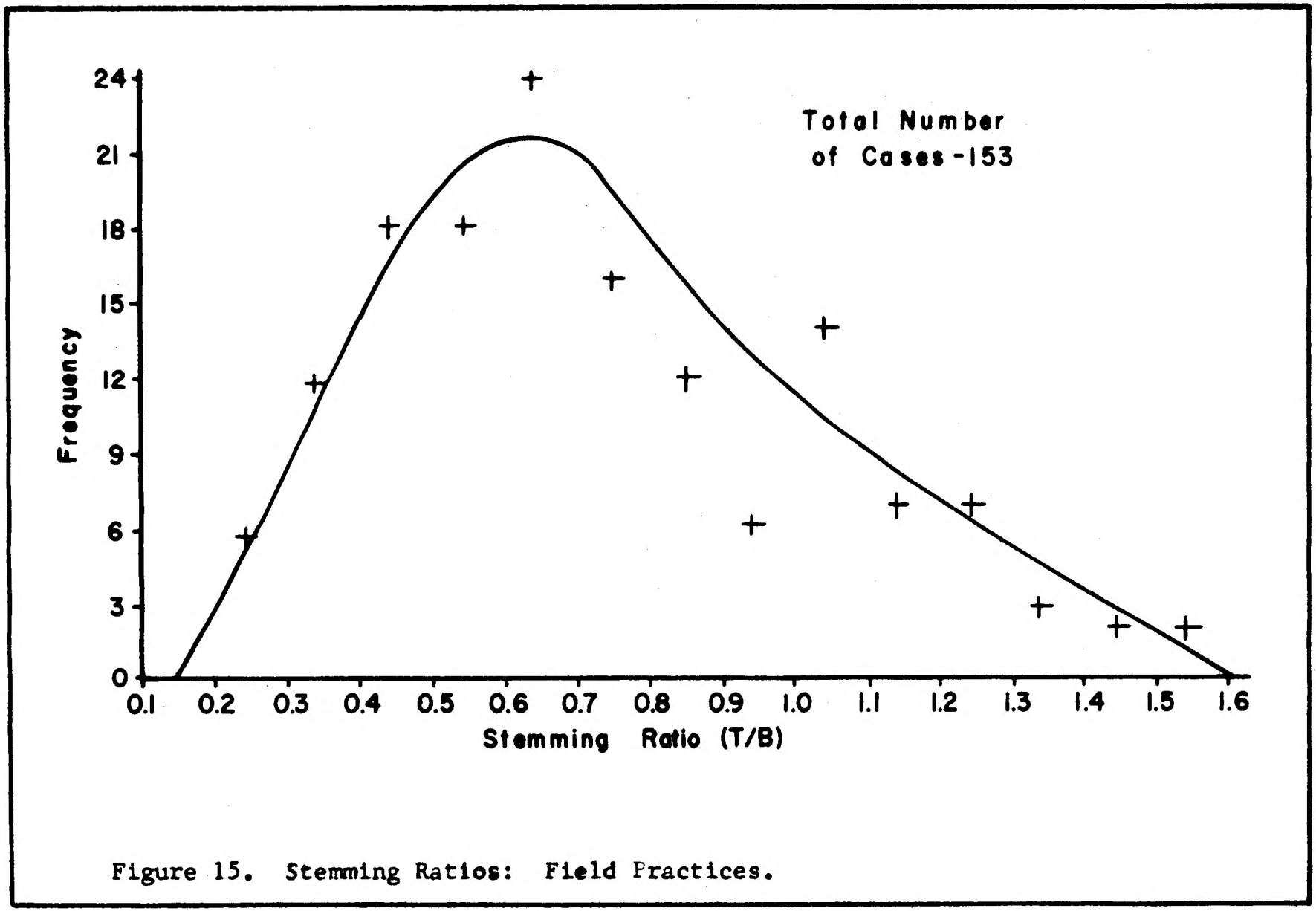

Figure 15. Stemming Ratios: Field Practices.

mean value was determined to be 0.735 while the median was found to be 0.683. Table I shows the distribution of the stemming ratio values with a group interval of 0.1. The arithmetic mean was calculated by use of the following equation:

$$M = \frac{\sum_{i=1}^{14} f_i \, m_i}{N} \qquad (22)$$

$$\text{Thus, } M = \frac{6\text{x}0.245 + 12\text{x}0.345 + 18\text{x}0.445 + 18\text{x}0.545 + 25\text{x}0.645}{152} + \frac{19\text{x}0.745 + 13\text{x}0.845 + 6\text{x}0.945 + 14\text{x}1.045 + 7\text{x}1.145}{152} + \frac{7\text{x}1.245 + 3\text{x}1.345 + 2\text{x}1.445 + 2\text{x}1.545}{152} = 0.735$$

The median group was determined by dividing the total number of cases by two, and then determining in which group this value falls. The existance of a uniform distribution of data within each group was assumed, and thus, the exact medium could be determined by proportioning. Thus,

$$\frac{N}{2} = \frac{152}{2} = 76$$

The median value is in the 0.645 group and was determined as follows:

$$M_d = 0.595 = \frac{22}{25} \text{ x } .1$$
$$= 0.595 \quad .088$$
$$= 0.683$$

The modal group is 0.645, and the exact modal value was found by interpolation, with the following equation:

$$M_o = y + \frac{f_2 \quad (i)}{f_1 + f_2} \qquad (23)$$

where: y - lower limit of the modal group,

f_1 - frequency of the group below the modal group,

f_2 - frequency of the group above the modal group,

TABLE I

FREQUENCY DISTRIBUTION OF STEMMING RATIO: FIELD PRACTICES

Stemming Ratio Group	Mid Point	Frequency
.20 - .29	0.245	6
.30 - .39	0.345	12
.40 - .49	0.445	18
.50 - .59	0.545	18
.60 - .69	0.645	25
.70 - .79	0.745	19
.80 - .89	0.845	13
.90 - .99	0.945	6
1.00 - 1.09	1.045	14
1.10 - 1.19	1.145	7
1.20 - 1.29	1.245	7
1.30 - 1.39	1.345	3
1.40 - 1.49	1.445	2
1.50 - 1.59	1.545	2

i - group interval.

Thus, $M_o = 0.60 \frac{19}{18 + 19} \times (0.1)$

$= 0.60\ 0.052$

$= 0.652$

In order for time-stress balancing to be achieved, the stemming ratio for a homogeneous, isotropic material should be one. However, the introduction of horizontal stratification planes in rock will tend to decrease the amount of energy that will reach the horizontal free face. If the rock in the vicinity of the collar of the blast-hole is to be broken, the stemming ratio must be decreased, as is evidenced by the data on field practices.

A frequency plot of the subdrilling ratio as used in industry is shown by Figure 16. It was found that the median, mode, and mean values were close or ranging from 0.243 for the mode to 0.294 for the mean. Table II shows the distribution of subdrilling ratios with a group interval of 0.1.

The variation of L/B with Ve/Vr was investigated for bench heights from 5 to 260 feet, the results of which are illustrated by Figure 17. The longitudinal wave velocity was estimated according to the values shown in Table III. The minimum L/B line shown on Figure 17 was drawn using the modal values obtained for the subdrilling ratio and the stemming ratio. In no case was a L/B value less than the minimum value as predicted from theoretical considerations.

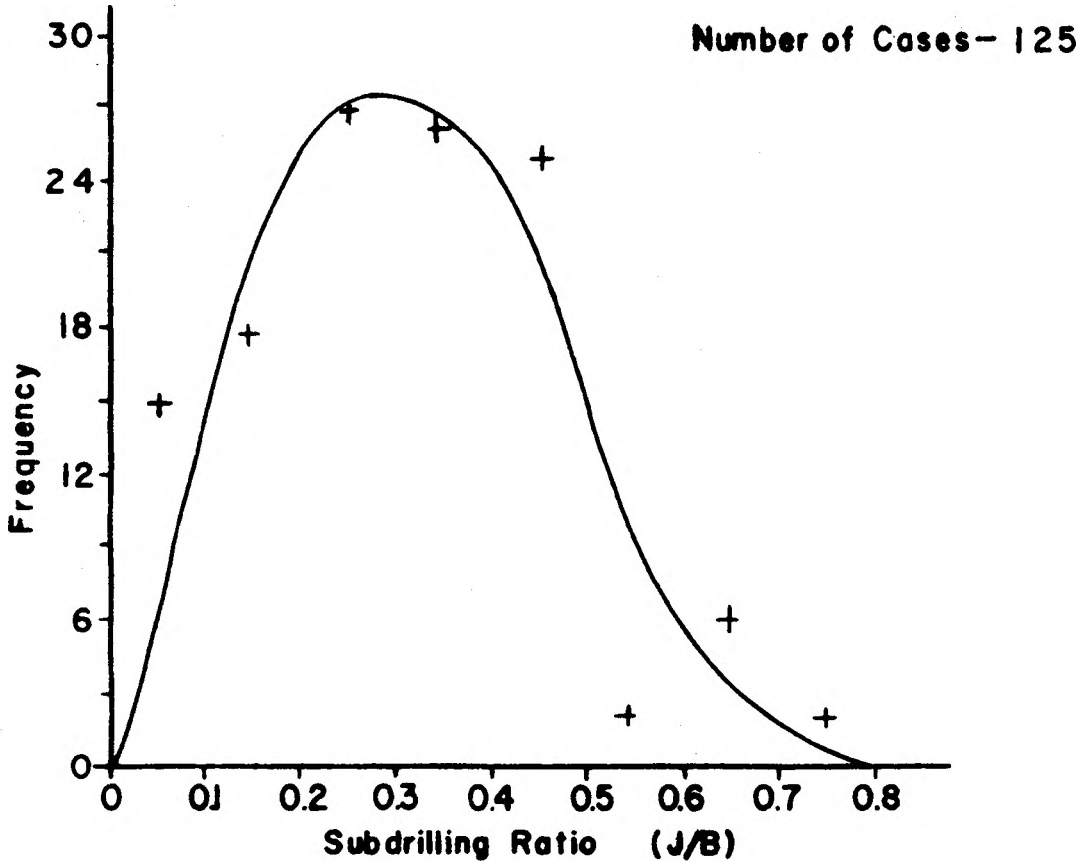

Figure 16. Subdrilling Ratios: Field Practices.

TABLE II

FREQUENCY DISTRIBUTION OF SUBDRILLING RATIO: FIELD PRACTICES

Subdrilling Ratio Group	Mid Point	Frequency
.0 - 0.09	0.045	15
0.1 - 0.19	0.145	18
0.2 - 0.29	0.245	27
0.3 - 0.39	0.345	26
0.4 - 0.49	0.445	25
0.5 - 0.59	0.545	2
0.6 - 0.69	0.645	6
0.7 - 0.79	0.745	2
0.8 - 0.89	0.845	0

TABLE III

SPEED OF TRANSMISSION OF LONGITUDINAL WAVES IN ROCKS*

Rock Type	Speed; ft/sec
Igneous Rocks	
Granite	13,400
Quartz Monozite	13,100
Diabase	21,300
Andesite	12,800
Sedimentary Rocks	
Limestone	12,000
Sandstone	8,200
Caliche	6,000
Rock Asphalt	5,000
Gypsum	9,800
Metamorphic Rocks	
Marble	14,000
Quartzite	19,000
Mica Schist	12,000

*After Peele, 1918, Mining Engineers' Handbook, John Wiley and Sons, Section 10a, p. 37.

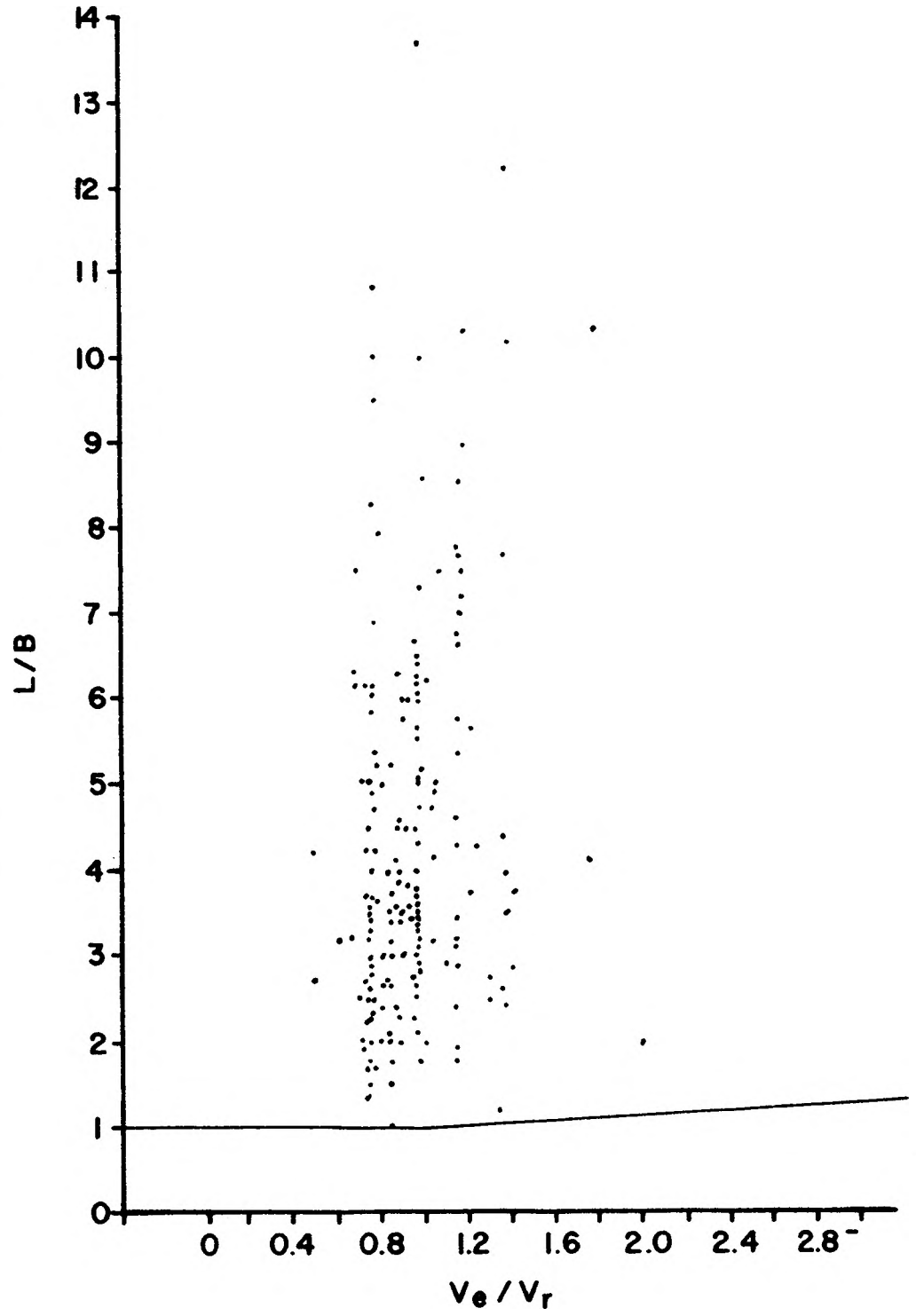

Figure 17. L/B vs. Ve/Vr: Field Practices.

The introduction of planes of weakness such as bedding planes and joints will necessitate corresponding modifications in the dimensions of the blast. Rock will break easier in definite directions according to its structure, and the explosive energy must be distributed to accommodate differing resistances to breakage offered by the rock. Thus, theoretical considerations should be modified to suit the particular conditions of a given blast.

CHAPTER V

SUMMARY AND CONCLUSIONS

The purpose of this investigation was to determine the following:

1. The importance of the explosive charge length on blasting effects when using vertical blast-holes,

and 2. The dependency of blast results on the detonation velocity of an explosive.

A literature search revealed that previous work on blasting was based on the assumption that the charge was concentrated at a single point, or that the detonation velocity of the explosive had an infinite value when a cylindrical charge was considered. Neither of these two assumptions are compatible with actual field blasting.

Mechanisms of impulsive energy transfer through rock were studied. Of particular interest were the effect of the pressure pulse on the medium through which it traveled, the characteristics of the pressure pulse and how they change with increasing travel distance, and the effects of density discontinuities in the rock on energy distribution patterns.

Stress distribution in rock is dependent on the detonation velocity and the detonation pressure of an explosive. The detonation pressure, on the other hand, appears to be primarily a function of the explosive

detonation velocity, and to a lesser degree, the explosive's density. Therefore, it would appear to be more desirable to relate the work potential of explosives in terms of their detonation velocities, rather than on the basis of densities, as is customarily practiced.

The position at which a cylindrical explosive charge is initiated and the direction of initiation largely determine the resulting generated stress-distribution patterns in rock. The nature of the ensuing blast would then be dependent on the primer position, all other factors being the same. In this respect, the influence on the stress distribution in rock was investigated for both collar priming and bottom priming. It was found that the velocity of the explosive, in relation to the velocity of wave propagation through the rock, largely determines the degree of time-stress balancing attained during blasting for any set of blast dimensions. If time-stress balancing is not achieved, adverse blast effects could result. Bottom primed blasts having a velocity ratio of less than one would often be violent. It is suggested that this effect could be expected because considerable prestressing and possible fracturing of rock occurs on the horizontal free face before the entire column of explosive has had time to react.

The charge length, and to a lesser degree the velocity ratio, determines the direction of the forces imparted into different positions in the rock. The forces

in the rock should be directed such that maximum utilization of the explosive energy can be realized.

A correlation of many field blasting practices appeared to validate the theoretical considerations. Therefore, from the results of this investigation the following conclusions are indicated:

1. A minimum height-to-burden ratio exists when bottom priming is employed, while a maximum height-to-burden ratio exists when a charge is collar primed. These ratios are both dependent on the velocity ratio. In no case should the burden dimension exceed the bench height.
2. If time-stress balancing is to be achieved, the stemming ratio should not exceed a value of one in the case of bottom priming, while it should never be less than one when collar priming is used. The magnitude of the forces in the rock around the collar will be unequally distributed unless the stemming ratio is one, regardless of the primer position. However, in the event of density discontinuites, the stemming ratio in both cases should be less than one to insure that sufficient energy is imparted to the rock around the collar of the blast-hole to cause satisfactory fragmentation. Because of this necessity to overcome energy losses those blasts that are collar primed may be more violent than those that are bottom primed.

3. The direction of the forces at different points in rock is largely dependent on the charge length, and to a lesser degree the velocity ratio. However, the direction of the forces must be such that rock breakage and movement can occur. The necessity of subdrilling when blasting in massive rock can be explained on the basis of force directions in the lower portion of the bench.

CHAPTER VI

PROPOSED AREAS FOR FUTURE INVESTIGATION

The conclusions reached from this investigation, although indicative of the importance of several factors involved in blasting, are only preliminary. In those areas that are not completely understood, such as the nature of explosive energy propagation through rock, the use of qualified assumptions was necessary. It would be of great value both to scientific researchers and to industry if a more complete knowledge of blasting processes could be acquired.

The effects of air spaces between an explosive and the walls of the blast-hole has been investigated (3). However, more research is needed to study the effect of the time delay in energy transmission across this gap and the subsequent stress patterns developed in the rock. The charge design itself should be further investigated to determine effects of air gaps between charges in the column (19).

Preliminary investigations indicate that the stresses generated from a cylindrical charge have a definite directional pattern. This directional effect, however, was not considered in this investigation because of a lack of accurate information. Blasting results may be strongly influenced by the directivity of the forces imparted to the rock. The directivity appears to be dependent on the

direction of detonation, and it is quite likely influenced by the mechanism of energy transfer from an explosive into the rock.

The validity of the theory of tensile slabbing has been well established both in the laboratory and by field observations. However, the importance of this mechanism in the fragmentation range desired during blasting, in relation to other modes of rock breakage, has not been thoroughly defined. It is possible that other forms of rock breakage may also be very important in bench blasting. It would be of value to determine exactly how the rock located just above the quarry floor is broken, and what effect the lateral restraint present below the quarry floor exerts on the breakage process. The effect of transverse stresses on rock breakage should also be investigated.

No attempt has been made in this investigation to define the proper burden dimension that can be applied to a given amount and type of explosive. Many factors are involved in such a determination, and the intensive research on the importance of these factors being conducted at the present time should be continued. It appears that the charge length is more important than previously considered, therefore, it is suggested that future investigations should be designed to determine the composite effects of bench height, the force distribution resulting from detonation of cylindrical charges, and static load-

ing on the results of blasting.

Geologic structures strongly influence the nature of energy transmission through rock. Density discontinuities disrupt the passage of pressure waves, causing them to be reflected and refracted. The interactions of incident, reflected, and refracted waves, and the resulting effects on blasting, should be investigated to enable the correlation of field observations and theoretical studies.

APPENDIXES

A. Table of Symbols

B. Derivation of Time-Stress Balancing Relationships

C. Graphical Method for Determining the Magnitude and Direction of the Resultant Forces at Different Points in a Medium from Detonation of a Cylindrical Charge

D. Sequence Photographs of Field Bench Blasts Using Large Diameter Vertical Blast-holes

A. Table of Symbols

α - covolume of gas at temperature and pressure of detonation.

α_o - covolume of gas at standard temperature and pressure.

a - constant relating covolume and density.

b - constant, for stress fall-time, and dependent of rock type.

B - burden dimension, or the distance between the charge and the nearest free face and measured in the direction of most probable displacement, in feet.

β - energy absorption constant of rock for increasing travel distance.

γ - $1 + \frac{nR}{c_v}$

C - constant, dependent of energy required to break rock.

C' - constant, dependent on the rock density.

c_v - specific heat of gaseous products at constant volume.

d_e - diameter of explosive charge, inches.

E - total energy content.

J - subdrilling, depth in feet, of the blast-hole below the quarry floor level.

K - constant, dependent on explosive amount and type.

^oK - temperature, degrees Kelvin.

L - bench, or ledge height, in feet.

n - number of moles of gaseous products per Kg of explosive.

P_d - explosive detonation pressure, psi.

P_o - initial explosive pressure, psi.

P_r - pressure generated at different points in the rock, psi.

R - gas constant.

ρ - density of explosive at any temperature and pressure gm/cc.

ρ_o - density of explosive at standard temperature and pressure gm/cc.

S_t - tensile strength of rock, psi.

T - stemming, in feet, that portion of a blast-hole between the hole collar and the explosive charge, and is generally filled with some inert confining material.

θ - angle between resultant wave front and blast-hole when Ve/Vr 1.

V - specific volume of gaseous products in the detonation head, cc/gm.

V_o - specific volume of undetonated explosive, cc/gm.

V_c - sonic wave velocity of a material, ft/sec.

V_e - detonation velocity, ft/sec.

V_r - longitudinal wave velocity of rock, ft/sec.

V_s - velocity of gaseous products behind detonation head, ft/sec.

W - constant, dependent on the wave length of the pulse.

x - travel distance, ft.

Z - characteristic impedance of a material, lb/ft^2 sec.

B. Derivation of Time-Stress Balancing Relationships

The detonation wave in an cylindrical explosive travels through the charge at a rate characteristic of the explosive type. The rock surrounding the charge is subjected to an intense pressure from the detonation which, in turn, causes a compressive wave to propagate outward through the rock in all directions. When the compressive wave reaches a free face, a reflected tensile wave is generated that travels back into the rock. Rock breakage in tension could then occur, resulting in cratering action. It is considered as desirable to have the cratering action uniform on all free faces, to prevent premature pressure relief in any one particular direction. When blasting with a cylindrical charge, it is impossible for the compressional wave from the entire charge to reach the total area of all free faces at the same time instant. Thus, a blast must be designed such that the first arrival of the compressional wave at the free faces will be at a location where the least undesirable blast effects will occur. When blasting with vertical cylindrical charges, the position in the rock that offers the most resistance to movement is along the base of a bench, or the toe. It is assumed then, that it is at that position where the compressional wave should arrive first.

Bottom Priming

The detonation wave in the explosive travels up the

charge when bottom priming is employed. The distribution of the stresses in the rock depends on the velocity ratio, and this distribution determines the relative arrival times of the compressive wave at each free face. If time-stress balancing is to be achieved, the first arrival must be at the base of the bench; the compressional pulse that first reaches this position usually originates from the bottom of the blast-hole. The travel time, then, from the bottom of the charge to the base of the bench must be equal to, or less than, the least travel time to the horizontal free face. This travel time would be (see Figure 18),

$$t_1 = \frac{(B^2 + J^2)^{\frac{1}{2}}}{V_r} \qquad (24)$$

The least travel time to the top of the bench is dependent on the velocity ratio. When this ratio is greater than one, the first pressure pulse to reach the horizontal free face at the top of the bench would be that from detonation at the top of the charge. In this case the travel distance in the rock would be equal to the stemming. The total travel time would equal the sum of the time required for the detonation wave to traverse the charge length and the travel time required for the compression wave in the rock to travel a distance equal to the stemming. The total travel time in the vertical direction can then be expressed as:

$$t_2 = \frac{PC}{V_e} + \frac{T}{V_r} = \frac{L - T + J}{V_e} + \frac{T}{V_r} \qquad (25)$$

Since t_2 must be greater than t_1, the limiting condition

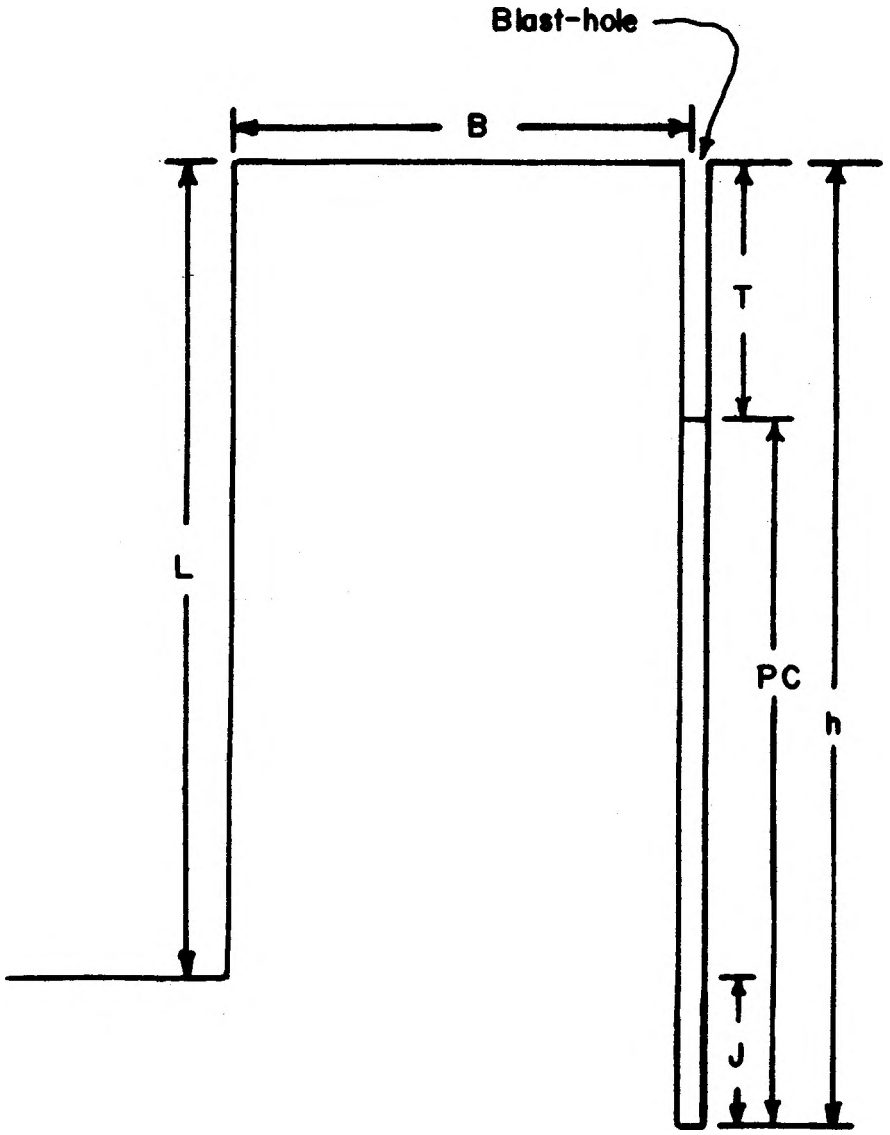

Figure 18. Vertical Bench Section Illustrating Blast Geometry.

for time-stress balancing is when $t_1 = t_2$. Thus,

$$\frac{(B^2 + J^2)^{\frac{1}{2}}}{V_r} = \frac{L - T + J}{V_e} + \frac{T}{V_r} \tag{26}$$

Solving for L and dividing through by B yields

$$\frac{L}{B} = \frac{T}{B}\left[1 - \frac{V_e}{V_r}\right] + \frac{V_e}{V_r}\left[1 + \left(\frac{J}{B}\right)^2\right]^{\frac{1}{2}} - \frac{J}{B}, \tag{27}$$

which is the desired solution.

When the velocity ratio is less than one, the first compressional wave to reach the top of the bench results from detonation at the base of the charge (see Figure 4a). The compressional wave travels through the rock at the rate of compressive energy propagation of the rock for a distance equal to the hole depth. Thus, the shortest travel time to the top of the bench is

$$t_3 = \frac{H}{V_r} = \frac{L + J}{V_r}, \tag{28}$$

while the shortest travel time to the base of the bench is as expressed in Equation 24. Equating the two travel times as before gives

$$\frac{(B^2 + J^2)^{\frac{1}{2}}}{V_r} = \frac{L + J}{V_r}, \tag{29}$$

which when solved for L and dividing through by B yields

$$\frac{L}{B} = \left[1 + \left(\frac{J}{B}\right)^2\right]^{\frac{1}{2}} - \frac{J}{B} \tag{30}$$

It should be noted that neither the detonation velocity of the explosive nor the stemming ratio is considered in Equation 30. Thus, when the velocity ratio is less than one, the minimum L/B ratio is independent of the velocity

of the explosive and is equal to one when J/B equals 0.

When the velocity ratio equals one, Equation 27 reduces to Equation 30, as would be expected.

Collar Priming

When a cylindrical charge is collar primed, the detonation wave proceeds down the explosive charge generating a compressive pulse in the rock that travels outward in all directions. The generated compressive pulse will first reach the vertical free face at a point directly out from the point of initiation. The first generated reflected-tensile-wave will form at this position, resulting in the formation of a tensile fracture that will propagate both up the free face to the top of the bench and down it to the base of the free face. However, since the magnitude of the stresses along the compressive pulse front decays very rapidly with travel distance, the component of the pulse from the upper portion of the charge is small at the base of the free face. The rock at the base of the bench then, would be more likely broken by the stresses developed from the detonation of the explosive at the lower portion on the blast-hole. Thus, as a limiting condition it can be assumed that the detonation of the explosive at the bottom of the blast-hole is responsible for rock breakage at the base of the bench.

Time-stress balancing demands that the rock at the base of the vertical free face be broken prior to, or

simultaneously with, that at the top of the bench. The travel distance to the top of the bench is equal to the stemming, and the travel time in this direction is then equal to

$$t_4 = \frac{T}{V_r} \tag{31}$$

Assuming as the limiting condition that the rock at the base of the bench is broken by the explosive at the bottom of the blast-hole, the travel time from the point of initiation to the base of the bench then equals

$$t_5 = \frac{PC}{V_e} + \frac{(B^2 + J^2)^{\frac{1}{2}}}{V_r} \tag{32}$$

Equating the two travel times, solving for L and dividing by B yields

$$\frac{L}{B} = \frac{T}{B}\left[1 + \frac{V_e}{V_r}\right] - \frac{V_e}{V_r}\left[1 + \left(\frac{J}{B}^2\right)\right]^{\frac{1}{2}} - \frac{J}{B} \tag{33}$$

The L/B ratio for collar priming as described in the above equation is the maximum value that can be used for time-stress balancing. Beyond this maximum value stressing and possible fracturing will occur at the top of the bench before it occurs at the base, which could result in cratering, overbreak, and flyrock at the top of the bench.

C. Graphical Method for Determining the Magnitude and Direction of the Resultant Forces at Different Points in a Medium From Detonation of a Cylindrical Charge

The detonation of an explosive in a material forms a pressure wave that diverges outward into the medium. The maximum force in the medium, which is along the wave front, decays approximately as the inverse square of the travel distance in rock-like materials. The amplitude of a force delivered to a point in the material then depends on the distance of the point from the explosive charge. The pulse shape, however, determines how the magnitude of the force will decrease as the pulse travels past the point. It appears that the pulse shape in rock very nearly approximates a triangle, and that the pulse length does not increase substantially for the travel distance ranges encountered in blasting. As the pulse passes a point in the rock the magnitude of the force will decrease according to the shape of the pulse. As an explosive has a definite detonation velocity there is a time lag between the instant of initiation at one end of the charge and detonation of the explosive at the other end. Each point along the explosive charge, as each detonates, contributes to the force field in the medium around the charge. Thus, not only the travel distance and the pulse shape, but also the explosive velocity and charge length should be considered when deter-

mining the total force magnitude and direction at a point in the medium that results from detonation of a cylindrical charge.

The magnitude and direction of the forces at different points in the medium were determined, to the first approximation, by assuming that the charge length was composed of a continuous series of discrete point charges, from each of which diverged a spherical pulse of equal intensity in all directions.

As tensile breakage would occur along the reflected wave front, the magnitude and direction of the forces along this wave front were of particular interest. The analysis has thus been confined to investigating changes of magnitude and direction of the forces along the reflected wave front.

The convention adopted in this analysis was that the direction of the forces along a compressional wave front were perpendicular to the front and outward from the charge position. The forces along the reflected wave front were also assumed to be perpendicular to the wave front. The direction in which they act was determined by considering the boundary conditions at the free face. The sum of the stresses parallel to the free face must be equal to zero at the boundary since a fluid, such as air, cannot support a shearing stress. Thus, the forces along the reflected wave front would then act in a direction opposite the direction of divergence of the wave.

In the analysis the charge length was divided into a discrete number of point charges, from which the distribution of the wave fronts in the material was constructed for different velocity ratios (see Figure 4). A free face, parallel to the charge length, was located such that the reflected pulse from the point of initiation just reached the base of the blast-hole, as shown in Figure 19. Since only a discrete number of points along the explosive charge was considered, it was necessary to study solely the forces at points where the reflected wave was intersected by compressional fronts. In this way the resultant forces, as determined from the analysis, at different points in the material could be compared.

If tensile slabbing, or breakage, is to proceed back to the blast-hole the pulse length must at least be equal to twice the burden dimension, and this length was used in the analysis.

The total force at a point in the materials, at any time instant, is the vector sum of all the forces from different points along the explosive charge, and as such can be determined graphically. A force diagram, indicating the directions but not the magnitudes, was constructed for for each point in the material studied. The direction of the force from each point along the explosive charge that had reached the point in the material at the specific time instant and the direction of the force of the tensile wave were considered.

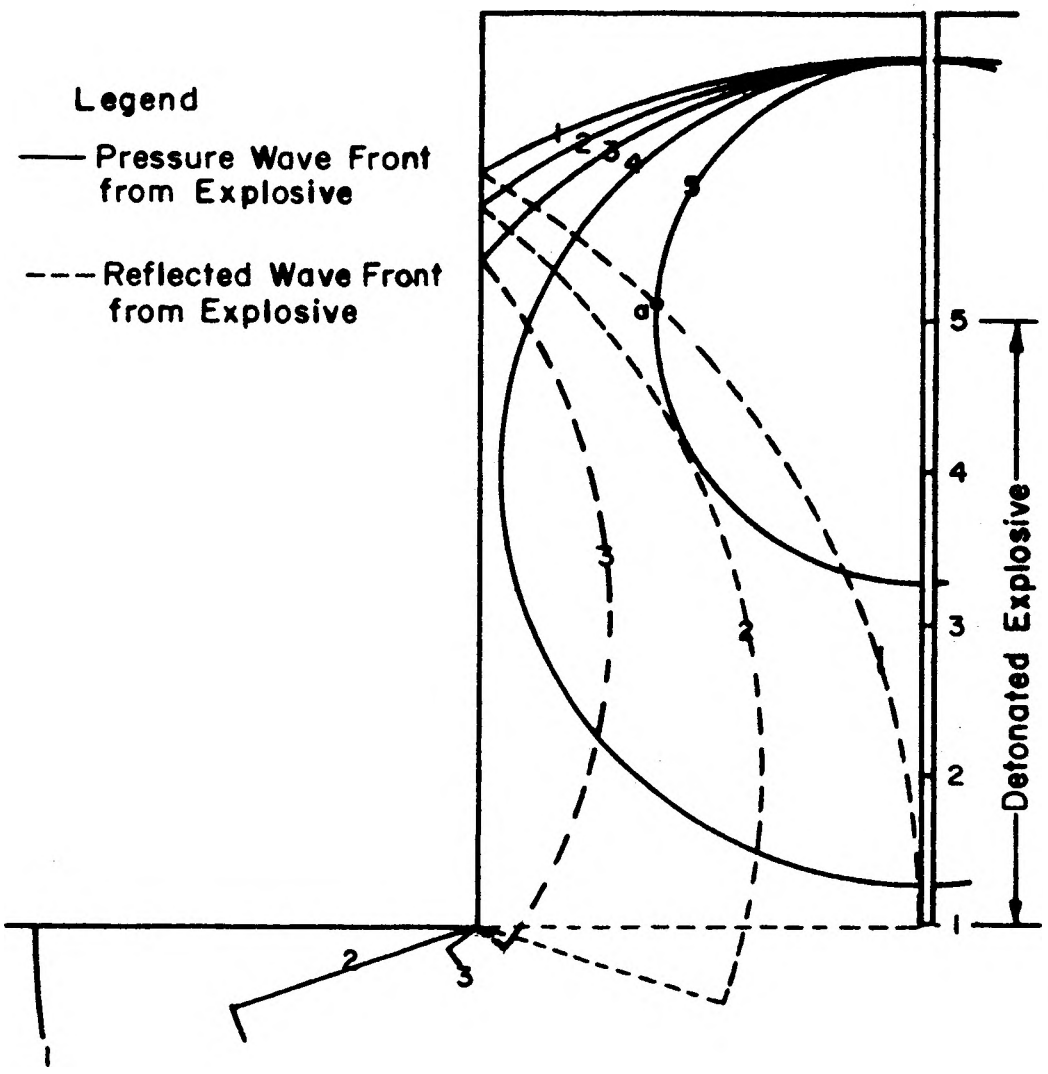

Figure 19. Simplified Distribution of Pressure Wave Fronts: Bottom Primed - Ve/Vr = 1.

The magnitude of each force was then determined by considering the travel distance and the pulse shape. A plot showing the rate of decay of the peak pressure (along the wave front) with increasing travel distance is shown in Figure 20. From this plot the peak pressure of the pulses from different points along the explosive charge, at the time instant of the analysis, was determined. It was found that the plot could be most conveniently used by overlaying it on Figure 19, such that the zero travel distance point was directly above the point in the explosive and that the point in the material being studied was overlain by the distance scale. The peak pressure, or force, was located where the wave front from the point in the charge intersects the overlain curve. When the point in the rock was behind the wave front, the force component due to the pressure wave was found by constructing the wave shape (pulse length = 2B). The force, resulting from detonation of the point in the charge, that was acting on the point in the material at that time instant was then found by measuring the height of the triangle above the point in the material. This operation is shown in Figure 21.

The above outlined procedure was then repeated for the same point in the medium for each point charge along the charge length. In a similar manner the magnitude of the forces at other points in the medium was then determined.

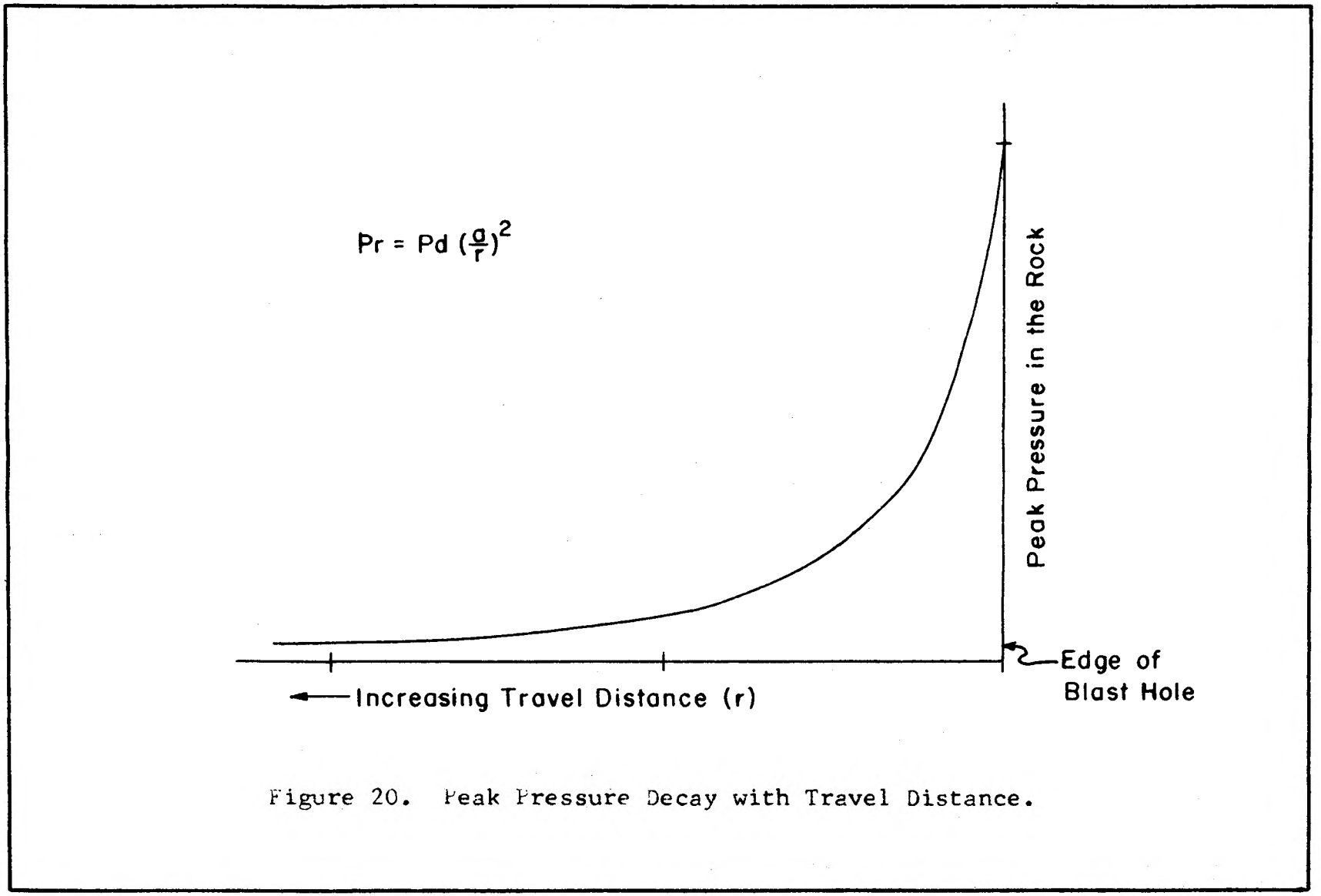

Figure 20. Peak Pressure Decay with Travel Distance.

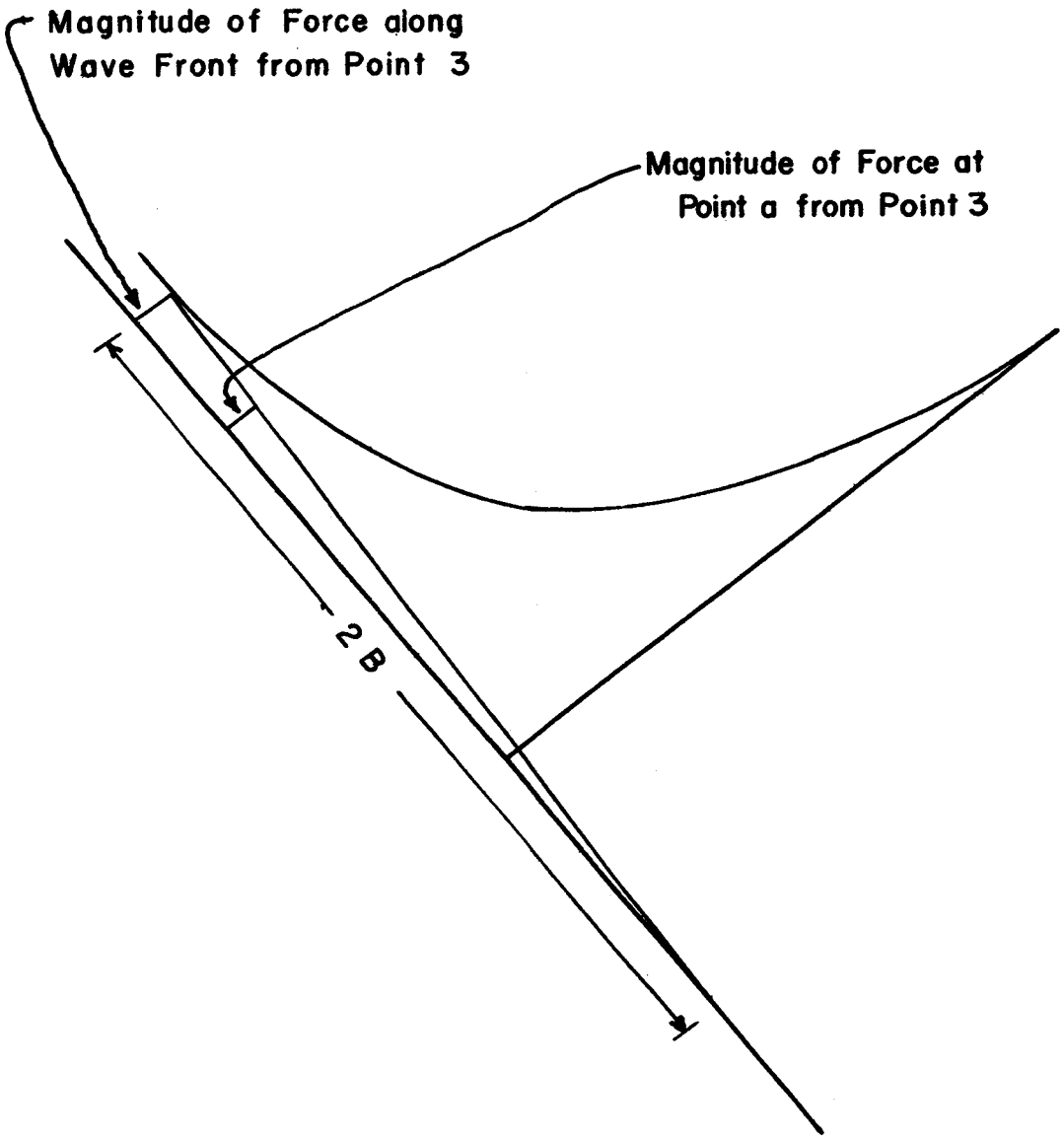
Magnitude of Force along
Wave Front from Point 3
Magnitude of Force at
Point a from Point 3
2B

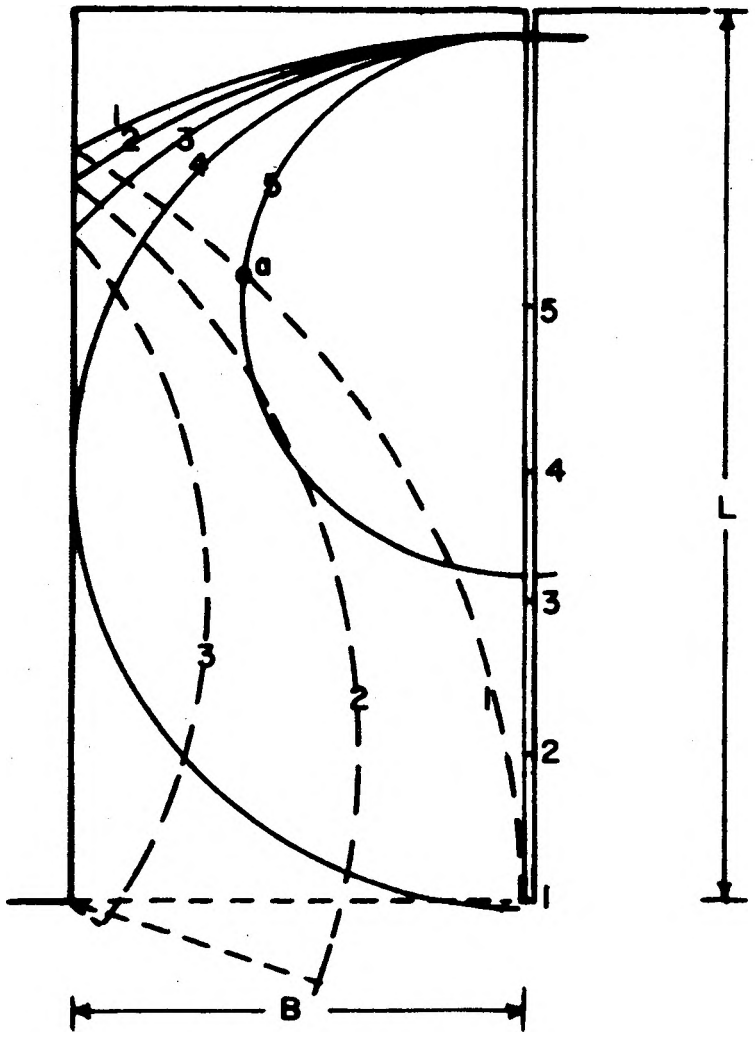

Figure 21. Graphical Determination of Force Magnitude at a point in Rock.

Using the force diagram and the magnitude of each force, the resultant magnitude and direction of the total resultant force was determined by constructing a force polygon, using standard mechanics techniques.

D. Sequence Photographs of Bench Blasts Using Large Diameter Vertical Blast-holes

In order to illustrate certain blasting phenomena described by this thesis visual observation of selected blasts made by industry are included.

The first set of photographs (Plate 7) shows the formation of a corner fracture shortly after initiation of a collar primed blast. The increase in fly-rock velocity in the upper and middle portions of the vertical face can be easily seen. The characteristic effects from bottom primed blasts are illustrated by Plate 8. The interaction of force components is readily detectable, and the bulging of the burden in hemispherical shapes in front of the blast-holes is clearly indicated. The movement of broken rock near the floor level before that from the upper portion of the bench face can also be observed. The absence of flyrock and lack of release of explosive gaseous products in the stemming regions are apparent from the photographs. On the other hand, Plate 9 shows the effects from collar priming for a relatively shallow bench. It should be noted that there is an almost immediate release of gaseous products along with the discharge of stemming at the time of charge initiation. Stressing in the collar region preceeds that in the lower portions of the bench, the action of which is more clearly detected for larger bench heights as shown by Plate 7,

as is the characteristic early release of stemming and explosive gaseous products.

CORNER FRACTURE FORMATION
QUARRY FACE BEFORE INITIATION
COURTESY OF ATLAS POWDER COMPANY

Plate 7a

300 ms. AFTER INITIATION

Plate 7b

600 ms. AFTER INITIATION

Plate 7c

900 ms. AFTER INITIATION

Plate 7d

BLASTING SEQUENCE FOR BOTTOM PRIMING
QUARRY FACE BEFORE INITIATION
COURTESY OF ATLAS POWDER COMPANY

Plate 8a

300 ms. AFTER INITIATION

Plate 8b

600 ms. AFTER INITIATION

Plate 8c

900 ms. AFTER INITIATION

Plate 8d

BLASTING SEQUENCE FOR COLLAR PRIMING
QUARRY FACE BEFORE INITIATION
COURTESY OF ATLAS POWDER COMPANY

Plate 9a

300 ms. AFTER INITIATION

Plate 9b

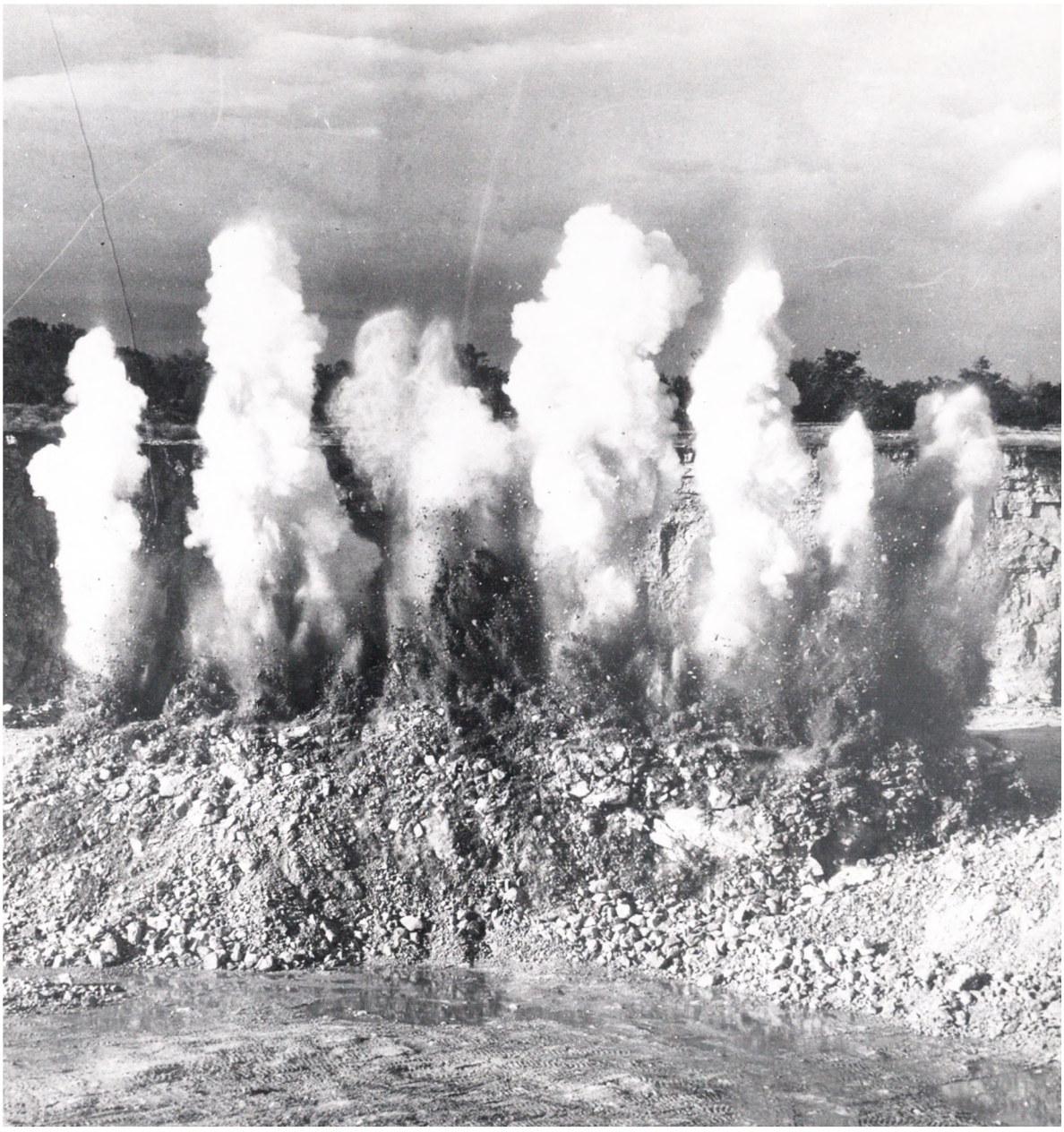

600 ms. AFTER INITIATION

Plate 9c

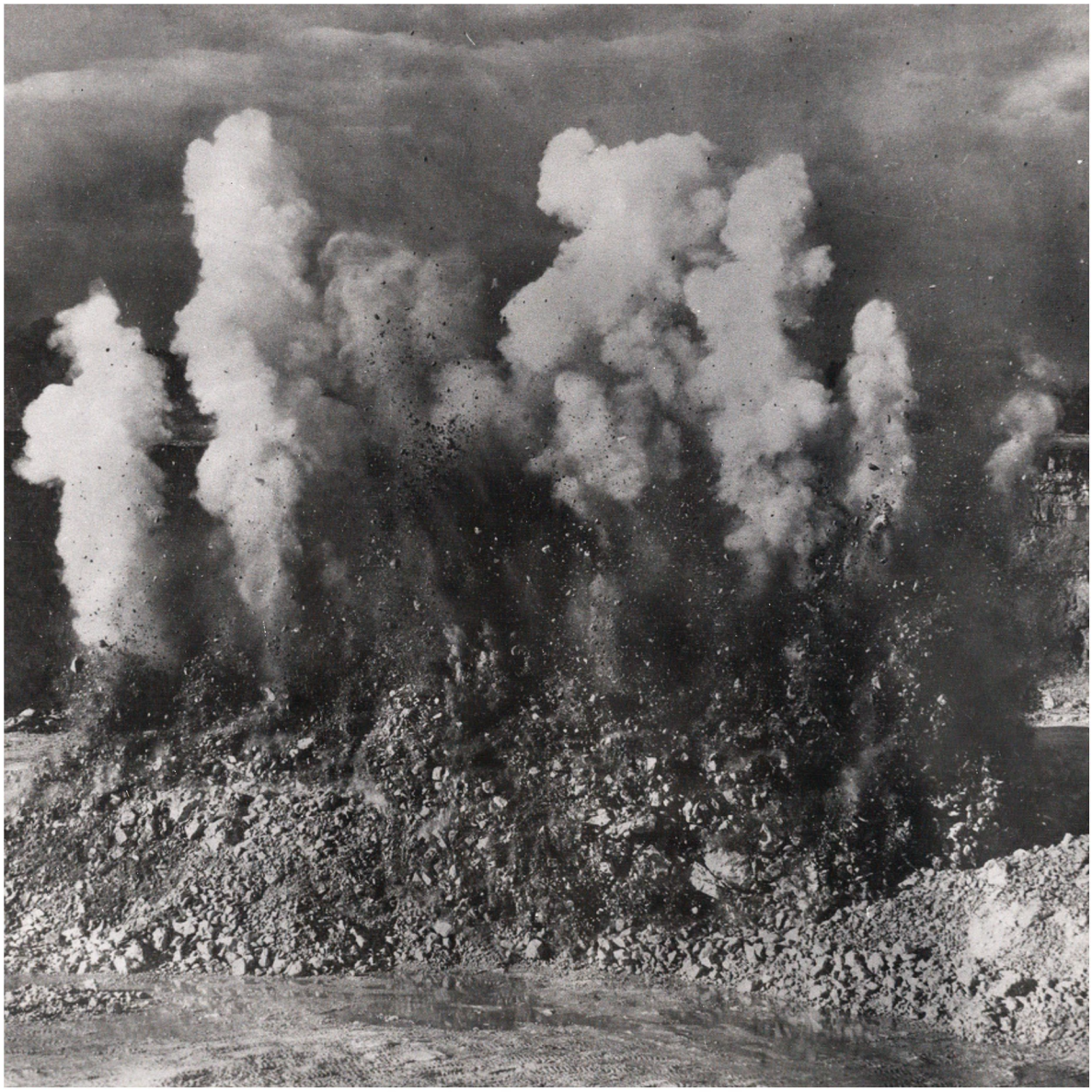

900 ms. AFTER INITIATION

Plate 9d

BIBLIOGRAPHY

BIBLIOGRAPHY

1. Anderson, 1952, Blast Hole Burden Design - Introducing a Formula, Proc. Australian Institute of Mining and Metallurgy, Vol. 166-167.

2. Ash, 1961, Drill Pattern and Initiation-Timing Relationships for Multiple-Hole Blasting, Quarterly of the Colorado School of Mines, Vol. 56, Number 1.

3. Atchison, 1961, Effects of Coupling on Explosive Performance, Quarterly of the Colorado School of Mines, Vol. 56, Number 1.

4. _____, and Tournay, 1959, Comparative Studies of Explosives in Granite, U. S. Bureau of Mines, RI 5509.

5. Baur, 1961, Application of the Livingston Theory, Quarterly of the Colorado School of Mines, Vol. 56, Number 1.

6. Bruzewski, Clark, Yancik, Kohler, 1959, An Investigation of Some Basic Performance Parameters on AN explosives, University of Missouri, School of Mines and Metallurgy, Technical Bulletin No. 97.

7. Clark, 1959, Mathematics of Explosive Calculations, University of Missouri, School of Mines and Metallurgy, Technical Bulletin No. 97.

8. Cook, 1958, Science of High Explosives, American Chemical Society, Monograph Series, Reinhold Publishing Co., New York, 440 p.

9. Duval, 1953, Strain Wave Shapes in Rock Near Explosives, Geophysics, Vol. XVIII, No. 2.

10. _____, 1959, Spherical Propagation of Explosion Generated Strain Pulses, University of Missouri, School of Mines and Metallurgy, Technical Bulletin No. 97.

11. _____, and Atchison, 1957, Rock Breakage by Explosives, U. S. Bureau of Mines, RI 5356.

12. Hino, 1959, Theory and Practice of Blasting, Nippon Kayaku Co., Ltd., Japan.

13. Ito, and Sassa, 1962, On The Detonation Pressure Produced at the Inner Surface of a Charge Hole, International Symposium on Mining Research, Proceedings of a Symposium Held at the University of Missouri, School of Mines and Metallurgy, Pergamon Press.

14. Kim, 1960, A Laboratory Study in Rock Fragmentation in Bench Blasting, Thesis, College of Mineral Industries, Pennsylvania State University.

15. Kinsler and Frey, 1950, Fundamentals of Acoustics, John Wiley and Sons, New York.

16. Kochanowsky, 1955, Blasting Research Leads to New Theories and Reductions in Blasting Costs, A. I. M. E., Trans. Vol. 202.

17. Langefors, 1959, Calculation of Charge and Scale Model Trials, Quarterly of the Colorado School of Mines, Vol. 54, No. 3.

18. Livingston, 1956, Fundamental Concepts of Rock Failure, Quarterly of the Colorado School of Mines, Vol. 51, No. 3.

19. Melnikov, 1962, Influence of Explosive Charge Design on Results of Blasting, University of Missouri, School of Mines and Metallurgy, International Symposium on Mining Research, Proceedings of Symposium, Vol. 1, Pergamon Press.

20. Mills, 1924, Statistical Methods, Henry Holt and Company, New York.

21. Nunley, 1960, Transmission of Plane Elastic Waves Through Layered Media, Thesis, The University of Tulsa.

22. Obert, and Duval, 1950, Generation and Propagation of Strain Waves in Rock, Part I, U. S. Bureau of Mines, RI 4683.

23. Paterson, 1947, The Hydrodynamic Theory of Detonation, Part II, On Absolute Calculations for Condensed Explosives, Research, Vol. 1.

24. Pearse, 1955, Rock Blasting, South African Mining and Engineering Journal, Vol. 66, Part I, No. 3243.

25. _____, 1955, Rock Blasting, Mine and Quarrying Engineering, Vol. 21, No. 1.

26. Petkof, Atchison and Duval, 1961, Photographic Observation of Quarry Blasting, U. S. Bureau of Mines, RI 5849.

27. Pickett, 1955, Siesmic Wave Propagation and Pressure Measurements Near Explosions, Quarterly of the Colorado School of Mines, Vol. 50, No. 4.

28. Ricker, 1953, The Form and Laws of Propagation of Seismic Wavelets, Geophysics, Vol. XVIII, No. 1.

29. Rinehart, 1958, Fracturing Under Impulsive Loading, University of Missouri, School of Mines and Metallurgy, Technical Bulletin, No. 95.

30. _____, 1959, The Role of Stress Waves in Comminution, Quarterly of the Colorado School of Mines, Vol. 54, No. 3.

31. Sharpe, 1942, The Production of Elastic Waves by Explosion Pressures, Geophysics, Vol. VIII, No. 3.

32. Taylor, 1952, Detonation in Condensed Explosives, Clarendon Press, Oxford, England.

33. Yancik and Clark, 1956, Experimentation with Large Hole Burn Cut Drift Rounds, University of Missouri, School of Mines and Metallurgy, Technical Bulletin No. 93.

34. Zeldovich and Kompaneets, 1960, Theory of Detonation, Academic Press, New York.

VITA

Thomas E. Pearse was born on July 9, 1938 at Boise, Idaho. He received his primary education at Tucson, Arizona, and his secondary education at Cairo, Egypt. In 1956 he was admitted to the New Mexico Institute of Mining and Technology, Socorro, New Mexico, and received the degree of Bachelor of Science in Geology in 1960. He was awarded a National Science Undergraduate Research Participation Program Scholarship for the academic year of 1959-1960.

In 1960 he enrolled in the Graduate School of the University of Missouri, School of Mines and Metallurgy, and at that time was appointed a graduate assistant.

His practical experience includes summer employment with the New Mexico Bureau of Mines and Mineral Resources, Socorro, New Mexico, and the Climax Molybdenum Company, Climax, Colorado.